WCAP-10861

ANALYSIS OF CAPSULE X FROM PORTLAND GENERAL ELECTRIC COMPANY TROJAN REACTOR VESSEL RADIATION SURVEILLANCE PROGRAM

S. E. Yanichko
S. L. Anderson
W. T. Kaiser

June 1985

APPROVED: _____

T. A. Meyer, Manager
Structural Materials and Reliability Technology

Work performed under Shop Order No. PMVJ-106

Prepared by Westinghouse Electric Corporation for the Portland General Electric Company

WESTINGHOUSE ELECTRIC CORPORATION
Nuclear Energy Systems
P. O. Box 355
Pittsburgh, Pennsylvania 15230

PREFACE

This report has been technically reviewed and verified.

- Sections 1 through 5,7 and 8 _____ R. S. Boggs

- Section 6 _____ A. H. Fero

- Appendix A _____ F. J. Witt

TABLE OF CONTENTS

LIST OF ILLUSTRATIONS

LIST OF ILLUSTRATIONS (cont)

LIST OF TABLES

LIST OF TABLES (cont)

SECTION 1
SUMMARY OF RESULTS

The analysis of the reactor vessel material contained in surveillance Capsule X, the second capsule to be removed from the Trojan reactor pressure vessel, led to the following conclusions:

- The capsule received an average fast neutron fluence ($E > 1.0$ MeV) of 1.77×10^{19} n/cm^2 while the maximum fluence at the vessel inner wall was 3.87×10^{18} n/cm^2.

- Irradiation of the reactor vessel lower shell plate C5583-1 to 1.77×10^{19} n/cm^2 resulted in 30 and 50 ft lb transition temperature increases of 95°F and 120°F, respectively, for specimens oriented normal to the principal rolling direction of the plate and 30 and 50 ft lb transition temperature increases of 90°F and 100°F, respectively for specimens oriented parallel to the plate principal rolling direction.

- Weld metal irradiated to 1.77×10^{19} n/cm^2 resulted in 30 and 50 ft lb transition temperature increases of 50°F and 55°F, respectively.

- Weld HAZ metal showed a 30°F and 50°F transition temperature increase of 60°F, after irradiation to 1.77×10^{19} n/cm^2.

- Plate C5583-1, weld metal, and HAZ metal all showed upper shelf energy levels well above 50 ft lb after irradiation to 1.77×10^{19}n/cm^2.

- The 30 ft lb transition temperature increases for the weld metal, weld HAZ and plate C5583-1 show that these materials are less sensitive to irradiation than predicted by Regulatory Guide 1.99 Revision 1.

- New plant heatup and cooldown limit curves were developed for 10 EFPY based on the capsule test results.

- The surveillance capsule removal schedule was revised as a result of the Capsule X evaluation.

SECTION 2
INTRODUCTION

This report presents the results of the examination of Capsule X, the second capsule to be removed from the reactor in the continuing surveillance program, which monitors the effects of neutron irradiation on the Trojan reactor pressure vessel materials under actual operating conditions.

The surveillance program for the Trojan reactor pressure vessel materials was designed and recommended by the Westinghouse Electric Corporation. A description of the surveillance program and the preirradiation mechanical properties of the reactor vessel materials are presented by Davidson and etal.[1] The surveillance program was planned to cover the 40-year design life of the reactor pressure vessel, and was based on ASTM E-185-73, "Recommended Practice for Surveillance Tests for Nuclear Reactor Vessels."[2] Westinghouse Nuclear Energy Systems personnel were contracted for the preparation of procedures for removing the capsule from the reactor and its shipment to the Westinghouse Research and Development Laboratory, where the postirradiation mechanical testing of the Charpy V-notch impact and tensile surveillance specimens were performed.

This report summarizes the testing of and the postirradiation data obtained from surveillance Capsule X removed from the Trojan reactor vessel and discusses the analysis of these data. The data are also compared to results of the previously removed Capsule U.[3]

SECTION 3
BACKGROUND

The ability of the large steel pressure vessel containing the reactor core and its primary coolant to resist fracture constitutes an important factor in ensuring safety in the nuclear industry. The beltline region of the reactor pressure vessel is the most critical region of the vessel because it is subjected to significant fast neutron bombardment. The overall effects of fast neutron irradiation on the mechanical properties of low alloy, ferritic pressure vessel steels such as SA 533 Grade B Class 1 (base material of the Trojan reactor pressure vessel beltline) are well-documented in the literature. Generally, low alloy ferritic materials show an increase in hardness and tensile properties and a decrease in ductility and toughness under certain conditions of irradiation.

A method for performing analyses to guard against fast fracture in reactor pressure vessels has been presented in "Protection Against Nonductile Failure," Appendix G, to Section III of the ASME Boiler and Pressure Vessel Code. The method utilizes fracture mechanics concepts is based on the reference nil-ductility temperature, RT_{NDT}.

RT_{NDT} is defined as the greater of the drop weight nil-ductility transition temperature (NDTT per ASTM E-208) or the temperature of 60°F less than the 50 ft-lb (and 35 mil lateral expansion) temperature as determined from Charpy specimens oriented normal (transverse) to the major working direction of the material. The RT_{NDT} of a given material is used to index that material to a reference stress intensity factor curve (K_{IR} curve) which appears in Appendix G of the ASME Code. The K_{IR} curve is a lower bound of dynamic, crack arrest, and static fracture toughness results obtained from several heats of pressure vessel steel. When a given material is indexed to the K_{IR} curve, allowable stress intensity factors can be obtained for this material as a function of temperature. Allowable operating limits can then be determined utilizing these allowable stress intensity factors.

RT_{NDT} and, in turn, the operating limits of nuclear power plants can be adjusted to account for the effects of radiation on the reactor vessel material properties. The radiation embrittlement of changes in mechanical properties of a given reactor pressure vessel

steel can be monitored by a reactor surveillance program such as the Trojan Reactor Vessel Radiation Surveillance Program,[1] in which a surveillance capsule is periodically removed from the operating nuclear reactor and the encapsulated specimens are tested. The increase in the average Charpy V-Notch 30 ft lb temperature (ΔRT_{NDT}) due to irradiation is added to the original RT_{NDT} to adjust the RT_{NDT} for radiation embrittlement. This adjusted RT_{NDT} (RT_{NDT} initial + ΔRT_{NDT}) is used to index the material to the K_{IR} curve and, in turn, to set operating limits for the nuclear power plant which take into account the effect of irradiation on the reactor vessel materials.

SECTION 4
DESCRIPTION OF PROGRAM

Six surveillance capsules for monitoring the effects of neutron exposure on the Trojan reactor pressure vessel core region material were inserted in the reactor vessel prior to initial plant startup. The six capsules were positioned in the reactor vessel between the neutron shielding pads and the vessel wall as shown in Figure 4-1. The vertical center of the capsules is opposite the vertical center of the core.

Capsule X was removed from the reactor after 4.28 Effective Full Power Years (EFPY) of plant operation. This capsule contained Charpy V-Notch, tensile, and Compact Tension (CT) specimens from submerged arc weld metal representative of the reactor vessel core region weld metal, and Charpy V-Notch, tensile, CT, and bend bar specimens from the lower shell plate C5583-1. The capsule also contained Charpy V-Notch specimens from weld Heat Affected Zone (HAZ) metal. All heat affected zone specimens were obtained from the weld HAZ of plate C5583-1. The chemistry and heat treatment of the program surveillance materials is presented in Table 4-1.

All test specimens were machined from the ¼-thickness location of the plates. Test specimens represent material taken at least one-plate thickness from the quenched end of the plate. Some base metal Charpy V-Notch and tensile specimens were oriented with the longitudinal axis of the specimens normal to (transverse orientation) and some parallel to (longitudinal orientation) the major working direction of the plate. The CT test specimens were machined so that the crack of the specimen would propagate normal to (longitudinal specimens) and parallel to (transverse specimens) the major working direction of the plate. All specimens were fatigue precracked per ASTM E399-72. The precracked bend bar was machined in the transverse orientation. Charpy V-Notch specimens from the weld metal were oriented with the longitudinal axis of the specimens normal to (transverse orientation) the weld direction. Tensile specimens were oriented with the longitudinal axis of the specimen normal to (transverse orientation) the weld direction.

Capsule X contained dosimeter wires of pure copper, iron, nickel, and aluminum-15% cobalt (cadmium-shielded and unshielded). In addition, cadmium-shielded dosimeters of Np^{237} and U^{238} were contained in the capsule.

Thermal monitors made from two low-melting-point eutectic alloys and sealed in Pyrex tubes were included in the capsule. The composition of the two alloys and their melting points are as follows:

2.5 percent Ag, 97.5 percent Pb	Melting point: 579°F (304°C)
1.75 percent Ag, 0.75 percent Sn, 97.5 percent Pb	Melting point: 590°F (312°C)

The arrangement of the various mechanical specimens, dosimeters and thermal monitors contained in Capsule X are shown in Figure 4-2.

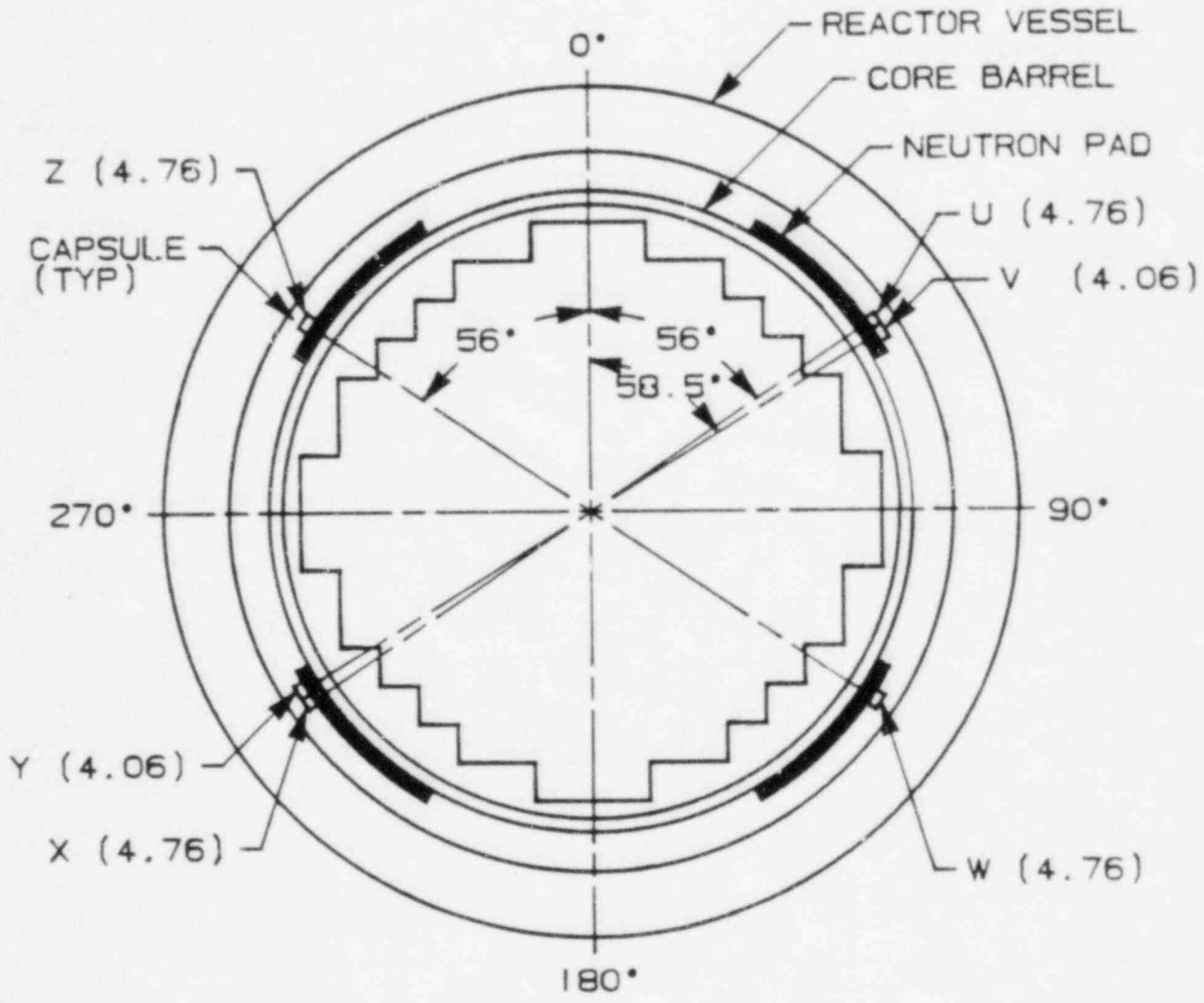

FIGURE 4-1. ARRANGEMENT OF SURVEILLANCE CAPSULES IN THE TROJAN REACTOR VESSEL
(UPDATED LEAD FACTORS FOR THE CAPSULES SHOWN INN PARENTHESES)

TABLE 4-1
CHEMISTRY AND HEAT TREATMENT OF MATERIAL REPRESENTING THE CORE REGION LOWER SHELL PLATE AND WELD METAL FROM THE TROJAN REACTOR VESSEL

CHEMICAL ANALYSIS (WEIGHT PERCENT)			
Element	Lower Shell Plate C5583-1	Weld Metal (a)	(b)
C	0.21	0.18	0.19
Mn	1.27	1.26	1.52
P	0.011	0.028	0.010
S	0.016	0.015	0.012
Si	0.20	0.54	0.35
Ni	0.60	0.93	0.97
Cr	0.048	0.058	0.09
V	0.002	0.002	< 0.010
Mo	0.53	0.51	0.50
Co	0.019	0.029	0.020
Cu	0.15	0.051	0.06
Sn	0.007	0.005	—
Al	0.021	0.009	0.020
N_2	0.007	0.010	—

HEAT TREATMENT	
Lower shell plate C5583-1	1650°/1750°F, for 5 hours, water quenched;
	1550°/1650°F, for 4½ hours, water quenched;
	1200°/1300°F, for 4¼ hours, air-cooled
	1100°/1175°F, for 36¾ hours, furnace-cooled
Weldment[c]	1100°/1175°F, for 9¾ hours, furnaced-cooled

a) Original analyis

b) Analysis on irradiated Charpy specimen PW50

c) Fabricated with Adcom Wire Heat No. S3986 and Linde 124 Flux Lot No. 934, which was used to fabricate the vessel beltline region intermediate to lower shell girth weld seams and the associated longitudinal weld seams.

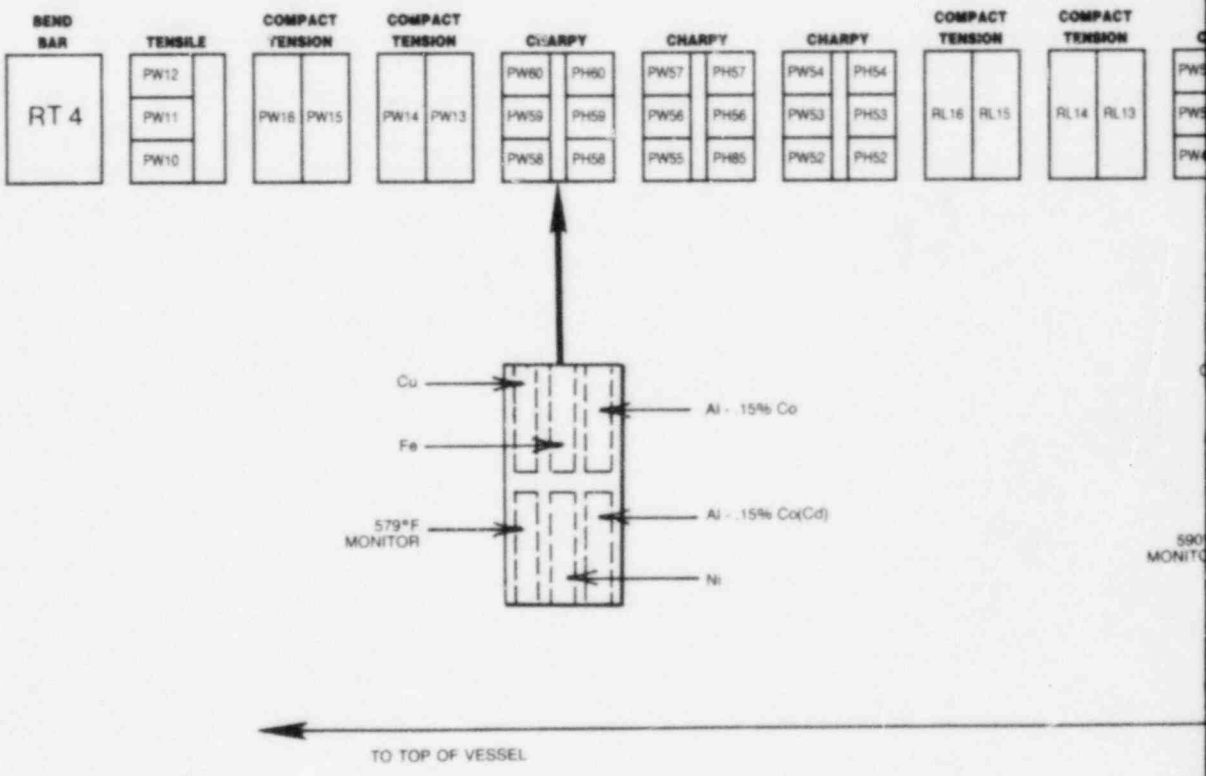
BEND BAR
RT 4
TENSILE
PW12
PW11
PW10
COMPACT TENSION
PW16
PW15
COMPACT TENSION
PW14
PW13
CHARPY
PW60
PW59
PW58
PH60
PH59
PH58
CHARPY
PW57
PW56
PW55
PH57
PH56
PH85
CHARPY
PW54
PW53
PW52
PH54
PH53
PH52
COMPACT TENSION
RL16
RL15
COMPACT TENSION
RL14
RL13
Cu
Fe
579°F MONITOR
Al - .15% Co
Al - .15% Co(Cd)
Ni
TO TOP OF VESSEL

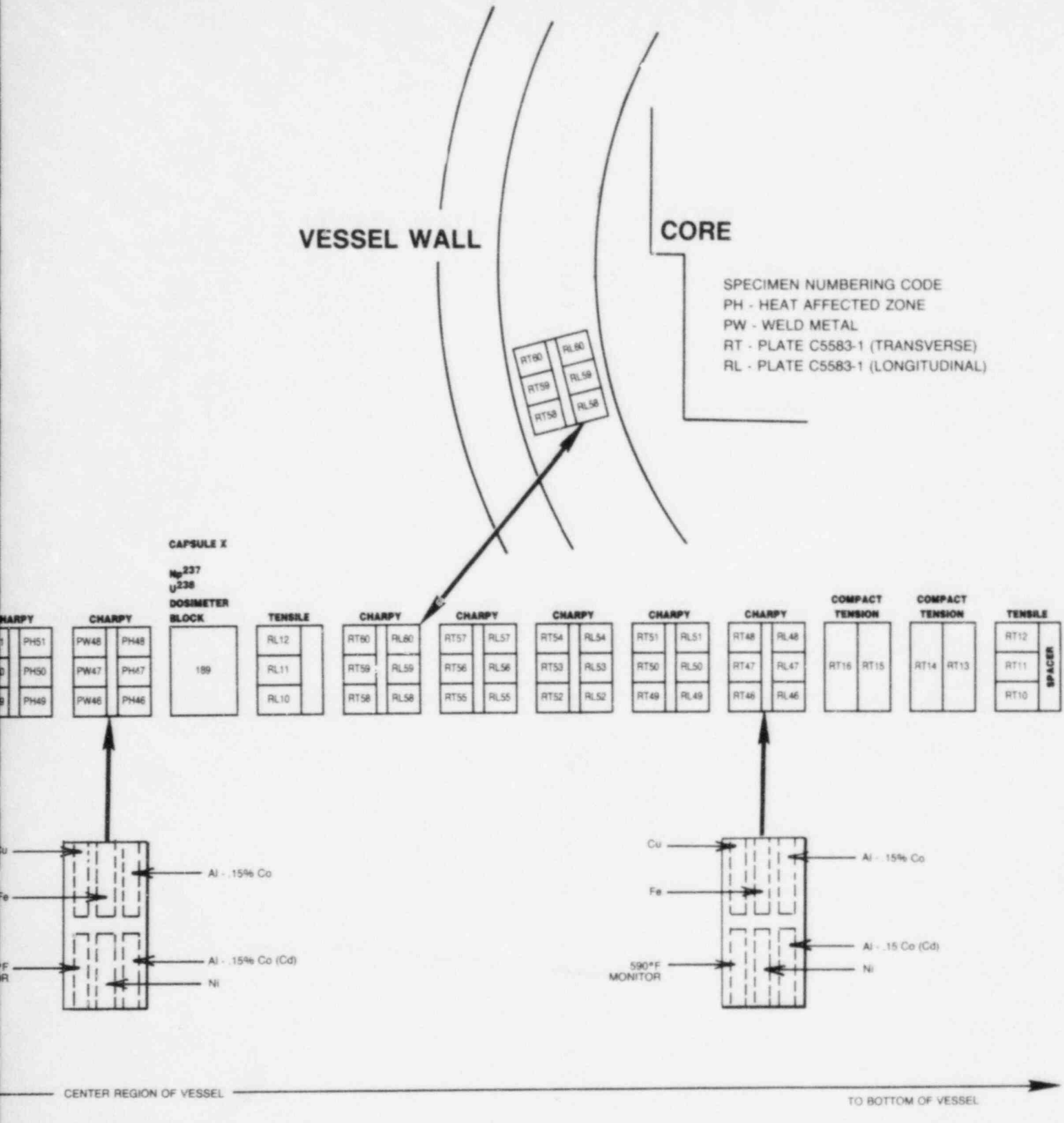

FIGURE 4-2. CAPSULE X DIAGRAM SHOWING LOCATION OF SPECIMENS, THERMAL MONITORS, AND DOSIMETERS

SECTION 5
TESTING OF SPECIMENS FROM CAPSULE X

5-1. OVERVIEW

The postirradiation mechanical testing of the Charpy V-Notch and tensile specimens was performed at the Westinghouse Research and Development Laboratory with consultation by Westinghouse Nuclear Energy Systems personnel. Testing was performed in accordance with 10CFR50, Appendices G and H, ASTM Specification E185-82, and Westinghouse Procedure RMF-8402, Revision 0.

Upon receipt of the capsule at the laboratory, the specimens and spacer blocks were carefully removed, inspected for identification number, and checked against the master list in WCAP-8426[1]. No discrepancies were found.

Examination of the two low-melting 304°C (579°F) and 310°C (590°F) eutectic alloys indicated no melting of either type of thermal monitor. Based on this examination, the maximum temperature to which the test specimens were exposed was less than 304°C (579°F).

The Charpy impact tests were performed per ASTM Specification E23-82 and RMF Procedure 8103 on a Tinius-Olsen Model 74, 358J machine. The tup (striker) of the Charpy machine is instrumented with an Effects Technology Model 500 instrumentation system. With this system, load-time and energy-time signals can be recorded in addition to the standard measurement of Charpy energy (E_D). From the load-time curve, the load of general yielding (P_{GY}), the time to general yielding (t_{GY}), the maximum load (P_M), and the time to maximum load (t_M) can be determined. Under some test conditions, a sharp drop in load indicative of fast fracture was observed. The load at which fast fracture was initiated is identified as the fast fracture load (P_F), and the load at which fast fracture terminated is identified as the arrest load (P_A).

The energy at maximum load (E_M) was determined by comparing the energy-time record and the load-time record. The energy at maximum load is roughly equivalent to the energy required to initiate a crack in the specimen.

Therefore, the propagation energy for the crack (E_p) is the difference between the total energy to fracture (E_D) and the energy at maximum load.

The yield stress (σ_y) is calculated from the three-point bend formula. The flow stress is calculated from the average of the yield and maximum loads, also using the three-point bend formula.

Percent shear was determined from postfracture photographs using the ratio-of-areas methods in compliance with ASTM Specification A370-77. The lateral expansion was measured using a dial gage rig similar to that shown in the same specification.

Tensile tests were performed on a 20,000-pound Instron, split-console test machine (Model 1115) per ASTM Specifications E8-81 and E21-79, and RMF Procedure 8102. All pull rods, grips, and pins were made of Inconel 718 hardened to R_C 45. The upper pull rod was connected through a universal joint to improve axiality of loading. The tests were conducted at a constant crosshead speed of 0.05 inches per minute throughout the test.

Deflection measurements were made with a linear variable displacement transducer (LVDT) extensometer. The extensometer knife edges were spring-loaded to the specimen and operated through specimen failure. The extensometer gage length is 1.00 inch. The extensometer is rated as Class B-2 per ASTM E83-67.

Elevated test temperatures were obtained with a three-zone electric resistance split-tube furnace with a 9-inch hot zone. All tests were conducted in air.

Because of the difficulty in remotely attaching a thermocouple directly to the specimen, the following procedure was used to monitor specimen temperature. Chromel-alumel thermocouples were inserted in shallow holes in the center and each end of the gage section of a dummy specimen and in each grip. In the test configuration, with a slight load on the specimen, a plot of specimen temperature versus upper and lower grip and controller temperatures was developed over the range room temperature to 550°F (288°C). The upper grip was used to control the furnace temperature. During the actual testing the grip temperatures were used to obtain desired specimen temperatures. Experiments indicated that this method is accurate to ± 2°F.

The yield load, ultimate load, fracture load, total elongation, and uniform elongation were determined directly from the load-extension curve. The yield strength, ultimate strength,

and fracture strength were calculated using the original cross-sectional area. The final diameter and final gage length were determined from post-fracture photographs. The fracture area used to calculate the fracture stress (true stress at fracture) and percent reduction in area was computed using the final diameter measurement.

5-2. CHARPY V-NOTCH IMPACT TEST RESULTS

The results of Charpy V-Notch impact tests performed on the various materials contained in Capsule X irradiated at 1.77×10^{19} n/cm^2 are presented in Tables 5-1 through 5-5 and Figures 5-1 through 5-4. The fractured surfaces of the impact specimens are shown in Figures 5-5 through 5-8.

Irradiation of Charpy V-Notch impact specimens from the reactor vessel lower shell plate, C5583-1, to 1.77×10^{19} n/cm^2 as shown in Figure 5-1 resulted in 30 and 50 ft lb transition temperature increases of 95°F and 120°F, respectively, for specimens oriented normal to the principal rolling direction (transverse orientation) of the plate. Specimens oriented parallel to the principal rolling direction (longitudinal orientation) of the plate as shown in Figure 5-2 exhibited 30 and 50 ft lb transition temperature increases of 90°F and 100°F respectively. The upper shelf energy of the shell plate showed a 8 ft lb decrease in the transverse direction and a 14 ft lb decrease in the longitudinal direction.

Weld metal specimens irradiated to 1.77×10^{19} n/cm^2 resulted in a 30 ft lb and 50 ft lb transition temperature increases of 50°F and 55°F, respectively, as shown in Figure 5-3. Irradiation did not cause any decrease in upper shelf energy.

Weld HAZ specimens irradiated to 1.77×10^{19} n/cm^2 resulted in a 30 ft lb and 50 ft lb transition temperature increase of 60°F as shown in Figure 5-4. The upper shelf energy of the HAZ metal decreased by 14 ft lb due to the irradiation.

Table 5-6 shows a summary of the Charpy test results for the two Capsules X and U tested to date. These results show that the higher fluence 1.77×10^{19} n/cm^2 received by Capsule X resulted in some additional increase in transition temperature and an additional decrease in shelf energy when compared with the Capsule U results.

Figure 5-9 shows a comparison of the actual increase in the 30 ft lb transition temperature versus the predicted increase based on Regulatory Guide 1.99 Revision 1[4] prediction methods for the Trojan vessel surveillance materials. These results show that the metals are less sensitive to radiation than predicted by the Guide.

The upper shelf energy values for the lower shell plate C5583-1 and the weld metal at 1.84×10^{19} n/cm^2 are greater than 50 ft lb as required by 10CFR50 Appendix G, Paragraph IV.A.1 and are predicted to exceed 50 ft lb throughout the design life of the vessel.

5-3. TENSION TEST RESULTS

The results of tension tests performed on material from the reactor vessel lower shell plate C5583-1 and weld metal irradiated to 1.77×10^{19} n/cm^2 are shown in Table 5-7 and Figures 5-10 through 5-12. Plate C5583-1 test results are shown in Figures 5-10 and 5-11 and indicate that irradiation to 1.77×10^{19} n/cm^2 caused a 15 ksi maximum increase in 0.2 percent yield strength and ultimate tensile strength. Weld metal tension test results presented in Figure 5-12 show that the 0.2 percent yield strength and ultimate tensile strength increased $\sim$ 7 ksi with irradition. The fractured tension specimens for the plate material are shown in Figures 5-13 and 5-14, while the fractured tension specimens for the weld metal are shown in Figure 5-15. A typical stress-strain curve for the tension tests is shown in Figure 5-16.

5-4. COMPACT TENSION TESTS

The ½T compact tension fracture mechanics specimens that were contained in Capsule X have not been tested and are stored at the Westinghouse Research Development Laboratory.

TABLE 5-1
CHARPY V-NOTCH IMPACT DATA FOR TROJAN PRESSURE VESSEL LOWER SHELL PLATE C5583-1 IRRADIATED AT 550°F, FLUENCE $1.77 \times 10^{19} n/cm^2$ (E > 1 MeV)

		Temperature		Impact Energy		Lateral Expansion		Shear
	Sample No.	(°F)	(°C)	(ft lb)	(J)	(mils)	(mm)	(%)
Longitudinal Orientation	RL50	0	– 18	10.0	13.5	9.5	0.24	1
	RL58	50	10	22.0	30.0	17.0	0.43	15
	RL53	60	16	25.0	34.0	19.5	0.50	18
	RL54	75	24	24.0	32.5	18.5	0.47	22
	RL56	75	24	46.0	62.5	29.5	0.75	29
	RL60	76	24	45.0	61.0	29.5	0.75	29
	RL46	100	38	43.0	58.5	29.5	0.75	24
	RL49	125	52	37.0	50.0	27.5	0.70	43
	RL51	125	52	50.0	68.0	33.5	0.85	47
	RL59	150	66	69.0	93.5	47.5	1.21	58
	RL55	175	79	61.0	82.5	47.0	1.19	65
	RL57	200	93	80.0	108.5	55.5	1.41	87
	RL52	225	107	101.0	137.0	67.5	1.71	100
	RL47	300	149	102.0	138.5	67.5	1.71	100
	RL48	350	177	103.0	139.5	72.0	1.83	100
Transverse Orientation	RT53	0	– 18	8.0	11.0	10.0	0.25	0
	RT49	75	24	22.0	30.0	16.0	0.41	16
	RT55	76	24	30.0	40.5	22.0	0.56	22
	RT54	100	38	31.0	42.0	20.0	0.51	24
	RT50	100	38	30.0	40.5	27.5	0.70	24
	RT56	125	52	30.0	40.5	27.5	0.70	36
	RT58	125	52	44.0	59.5	37.5	0.95	43
	RT46	150	66	44.0	59.5	38.0	0.97	50
	RT51	175	79	38.0	51.5	36.0	0.91	57
	RT52	200	93	55.0	74.5	48.5	1.23	76
	RT59	225	107	74.0	100.5	61.5	1.56	97
	RT47	250	121	85.0	115.0	57.5	1.46	98
	RT60	300	149	81.0	110.0	61.0	1.55	100
	RT48	350	177	65.0	88.0	53.0	1.35	100
	RT57	400	204	73.0	99.0	60.0	1.52	100

TABLE 5-2
CHARPY V-NOTCH IMPACT DATA FOR TROJAN PRESSURE VESSEL WELD METAL AND HAZ METAL IRRADIATED AT 550°F, FLUENCE $1.77 \times 10^{19} n/cm^2$ (E > 1 MeV)

	Sample No.	Temperature (°F)	Temperature (°C)	Impact Energy (ft lb)	Impact Energy (J)	Lateral Expansion (mils)	Lateral Expansion (mm)	Shear (%)
Weld Metal	PW59	-100	- 73	4.0	5.5	6.5	0.17	0
	PW52	- 50	- 46	18.0	24.5	12.5	0.32	6
	PW53	0	- 18	16.0	21.5	14.0	0.36	16
	PW55	25	- 4	27.0	36.5	23.5	0.60	32
	PW49	50	10	28.0	38.0	25.0	0.64	36
	PW57	50	10	31.0	42.0	26.5	0.67	47
	PW47	75	24	51.0	69.0	41.0	1.04	70
	PW50	77	25	38.0	51.5	32.0	0.81	62
	PW58	100	38	51.0	69.0	38.5	0.98	79
	PW48	125	52	65.0	88.0	53.0	1.35	87
	PW56	150	66	74.0	100.5	68.5	1.74	89
	PW54	200	93	58.0	78.5	56.0	1.42	94
	PW46	250	121	82.0	111.0	71.5	1.82	98
	PW51	300	149	84.0	114.0	70.0	1.78	100
	PW60	350	177	91.0	123.5	69.0	1.75	100
HAZ Metal	PH60	-100	- 73	12.0	16.5	11.5	0.29	8
	PH52	- 50	- 46	15.0	20.5	18.5	0.47	18
	PH55	- 50	- 46	41.0	55.5	25.0	0.64	18
	PH54	- 25	- 32	51.0	69.0	36.5	0.93	25
	PH59	0	- 18	29.0	39.5	18.0	0.46	30
	PH56	25	- 4	85.0	115.0	53.5	1.36	74
	PH58	25	- 4	16.0	21.5	19.5	0.50	24
	PH57	25	- 4	50.0	68.0	36.5	0.93	38
	PH47	50	10	50.0	68.0	34.5	0.88	54
	PH46	50	10	71.0	96.5	43.5	1.10	77
	PH50	75	24	109.0	148.0	69.0	1.75	95
	PH53	77	25	126.0	171.0	68.5	1.74	100
	PH49	150	66	97.0	131.5	64.5	1.64	100
	PH48	200	93	103.0	139.5	63.0	1.60	100
	PH51	300	149	120.0	162.5	76.0	1.93	100

TABLE 5-3
INSTRUMENTED CHARPY IMPACT TEST RESULTS FOR TROJAN REACTOR VESSEL LOWER SHELL PLATE C5583-1

	Sample Number	Test Temp (°F)	Charpy Energy (ft lb)	Normalized Energies (ft lbs/in²) Charpy Ed/A	Maximum Em/A	Prop Ep/A	Yield Load (kips)	Time to Yield (μSec)	Maximum Load (kips)	Time to Maximum (μSec)	Fracture Load (kips)	Arrest Load (kips)	Yield Stress (ksi)	Flow Stress (ksi)
Longitudinal Orientation	RL50	0	10.0	81	62	18	3.65	95	3.95	170	3.95		120	125
	RL58	50	22.0	177	137	40	3.50	95	4.20	320	4.15		116	128
	RL53	60	25.0	201	163	38	3.55	100	4.40	370	4.35		117	131
	RL54	75	24.0	193	115	78	3.50	90	4.20	275	4.20	0.55	115	127
	RL56	75	46.0	370	285	85	3.45	100	4.45	610	4.30	0.20	113	131
	RL60	76	45.0	362	282	81	3.45	100	4.50	600	4.20	0.40	115	132
	RL46	100	43.0	346	261	86	3.55	120	4.40	585	4.40	0.55	117	131
	RL49	125	37.0	298	197	101	3.35	100	4.40	445	4.20	1.00	111	128
	RL51	125	50.0	403	275	128	3.35	110	4.45	605	4.30	1.30	111	129
	RL59	150	69.0	556	262	294	3.40	120	4.30	605	3.85	2.05	112	127
	RL55	175	61.0	491	225	267	3.25	110	4.25	520	4.05	2.00	107	124
	RL57	200	80.0	644	264	381	3.05	105	4.20	610	3.75	2.50	101	120
	RL52	225	101.0	813	260	553	3.15	90	4.10	560			104	120
	RL47	300	102.0	821	259	562	2.90	95	4.20	595			96	118
	RL48	350	103.0	829	262	567	2.75	95	3.90	630			91	111
Transverse Orientation	RT53	0	8.0	64	42	22	3.75	100	3.90	130	3.85		124	127
	RT49	75	22.0	177	104	73	3.35	100	3.90	270	3.90	0.75	110	120
	RT55	76	30.0	242	178	63	3.40	100	4.30	410	4.30		112	127
	RT54	100	31.0	250	154	96	3.50	115	4.30	370	4.15	0.80	115	129
	RT50	100	30.0	242	137	105	3.40	105	4.10	335	3.90	0.80	113	124
	RT56	125	30.0	242	144	97	3.40	105	4.05	350	3.85	1.25	112	123
	RT58	125	44.0	354	220	134	3.20	105	4.20	510	4.15	1.45	106	122
	RT46	150	44.0	354	177	177	3.25	115	4.05	435	3.95	1.85	107	120
	RT51	175	38.0	306	140	166	3.25	95	3.95	345	3.90	2.00	107	119
	RT52	200	55.0	443	217	226	3.05	95	4.15	505	3.95	2.45	101	119
	RT59	225	74.0	596	187	408	3.15	130	3.95	485			105	117
	RT47	250	85.0	684	211	473	2.60	85	4.00	520			85	109
	RT60	300	81.0	652	225	427	2.80	85	3.95	535			93	112
	RT48	350	65.0	523	161	363	2.70	90	3.60	425			89	104
	RT57	400	73.0	588	166	422	2.70	120	3.65	455			89	105

TABLE 5-4
INSTRUMENTED CHARPY IMPACT TEST RESULTS FOR TROJAN REACTOR VESSEL WELD METAL AND HAZ METAL

	Sample Number	Test Temp (°F)	Charpy Energy (ft lb)	Normalized Energies (ft lbs/in²) Charpy Ed/A	Maximum Em/A	Prop Ep/A	Yield Load (kips)	Time to Yield (μ Sec)	Maximum Load (kips)	Time to Maximum (μ Sec)	Fracture Load (kips)	Arrest Load (kips)	Yield Stress (ksi)	Flow Stress (ksi)
Weld Metal	PW59	-100	4.0	32	20	12	2.95	75	3.20	85	3.20		98	102
	PW52	- 50	18.0	145	110	35	3.80	105	4.40	260	4.40		126	136
	PW53	0	16.0	129	68	61	3.55	95	3.95	185	3.95	0.30	117	124
	PW55	25	27.0	217	151	66	3.55	110	4.25	360	4.25	1.00	117	129
	PW49	50	28.0	225	150	76	3.30	90	4.20	350	4.20	1.30	110	124
	PW57	50	31.0	250	110	139	3.45	95	4.05	275	3.85	1.65	113	123
	PW47	75	51.0	411	200	211	3.35	95	4.15	460	3.90	2.30	110	123
	PW50	77	38.0	306	157	149	3.25	85	4.00	370	3.90	2.15	107	120
	PW58	100	51.0	411	215	196	3.40	100	4.20	485	4.20	2.40	112	126
	PW48	125	65.0	523	195	329	2.90	105	4.05	475			95	114
	PW56	150	74.0	596	207	389	3.30	120	4.05	495			110	122
	PW54	200	58.0	467	180	287	3.00	90	3.95	435			100	115
	PW46	250	82.0	660	221	439	2.95	90	4.05	520			97	116
	PW51	300	84.0	676	207	470	2.85	90	3.85	510			95	111
	PW60	350	91.0	733	235	498	2.85	85	3.90	560			95	112
HAZ Metal	PH60	-100	12.0	97	79	18	4.30	130	4.55	210	4.55		142	147
	PH52	- 50	15.0	121	83	38	3.90	95	4.35	200	4.20	0.20	130	137
	PH55	- 50	41.0	330	256	74	3.85	95	4.85	505	4.65		128	144
	PH54	- 25	51.0	411	261	150	3.90	110	4.85	525	4.70	0.35	130	145
	PH59	0	29.0	234	83	151	3.80	100	4.05	210	4.00	1.25	126	130
	PH58	25	16.0	129	40	89	3.60	110	3.85	135	3.65	0.90	119	123
	PH57	25	50.0	403	237	165	3.70	100	4.55	505	4.40	1.90	122	137
	PH56	25	85.0	684	270	415	3.85	115	4.60	560	3.75	2.20	127	139
	PH47	50	50.0	403	240	163	3.65	100	4.65	505	4.40	1.85	121	137
	PH46	50	71.0	572	246	326	3.60	90	4.55	510			119	135
	PH50	75	109.0	878	287	591	3.45	95	4.55	600			115	133
	PH53	77	126.0	1015	316	699	3.45	90	4.60	655			115	133
	PH49	150	97.0	781	276	505	3.25	95	4.30	610			107	125
	PH48	200	103.0	829	264	565	3.30	95	4.30	585			109	125
	PH51	300	120.0	966	306	660	2.95	100	4.20	695			98	119

TABLE 5-5
THE EFFECT OF 550°F IRRADIATION AT 1.77×10^{19}n/cm^2 (E > 1 MeV) ON NOTCH TOUGHNESS PROPERTIES OF TROJAN REACTOR VESSEL SURVEILLANCE MATERIALS

	Average 50 ft lb Temp (°F)			Average 35 mil Lateral Expansion Temp (°F)			Average 30 ft lb Temp (°F)			Average Energy Absorbtion at Full Shear (ft lb)		
Material	Unirradiated	Irradiated	ΔT	Unirradiated	Irradiated	ΔT	Unirradiated	Irradiated	ΔT	Unirradiated	Irradiated	Δ (ft lb)
Plate C5583-1 Transverse	50	170	120	32	142	110	8	103	95	84	76	− 8
Plate C5583-1 Longitudinal	20	120	100	15	120	105	− 15	75	90	116	102	− 14
Weld Metal	31	86	55	16	76	60	2	52	50	83	86	+ 3
HAZ Metal	− 37	23	60	− 40	25	65	− 57	3	60	125	111	− 14

TABLE 5-6
SUMMARY OF TROJAN REACTOR VESSEL SURVEILLANCE CAPSULE CHARPY IMPACT TEST RESULTS

Material	Capsule Ident.	Fluence n/cm²	30 ft lb Trans. Temp. Increase (°F)	30 ft lb Trans. Temp. Increase (°C)	50 ft lb Trans. Temp. Increase (°F)	50 ft lb Trans. Temp. Increase (°C)	Upper Shelf Energy Decrease (ft lb)	Upper Shelf Energy Decrease (J)
Plate C5583-1 (Longitudinal)	U	3.88×10^{18}	53	29	55	31	6	8
	X	1.77×10^{19}	90	50	100	56	14	19
Plate C5583-1 (Transverse)	U	3.88×10^{18}	44	24	65	36	0	0
	X	1.77×10^{19}	95	53	120	67	8	11
Weld Metal	U	3.88×10^{18}	22	12	32	18	2	3
	X	1.77×10^{19}	50	28	55	31	3[a]	4[a]
HAZ Metal	U	3.88×10^{18}	19	11	30	17	5	7
	X	1.77×10^{19}	60	33	60	33	14	19

a. Upper Shelf Energy Increase

TABLE 5-7
TENSILE PROPERTIES FOR TROJAN REACTOR VESSEL MATERIAL IRRADIATED AT 550°F TO 1.77×10^{19} n/cm (E > 1.0 MeV)

Specimen Number	Material	Test Temperature (°F)	0.2% Yield Strength (ksi)	Ultimate Strength (ksi)	Fracture Load (kip)	Fracture Stress (ksi)	Fracture Strength (ksi)	Uniform Elongation (%)	Total Elongation (%)	Reduction in Area (%)
RL12	Plate C5583-1 Longitudinal	125	82.2	102.7	3.50	178.5	71.3	9.8	20.4	60
RL11		225	75.4	95.7	3.34	170.4	68.0	10.5	20.4	60
RL10		550	73.3	96.8	3.75	171.2	76.4	9.4	18.7	55
RT12	Plate C5583-1 Transverse	125	84.0	100.8	3.75	212.2	76.4	9.9	19.4	64
RT10		225	77.4	95.7	3.50	147.2	71.3	9.6	17.4	52
RT11		550	71.3	93.7	3.90	160.3	79.5	9.3	16.0	50
PW11	Weld Metal	75	84.0	99.0	3.20	248.7	65.2	9.9	21.9	74
PW12		175	78.9	95.7	3.20	171.8	65.2	9.5	20.4	62
PW10		550	75.9	95.7	3.60	179.0	73.3	9.0	17.9	59

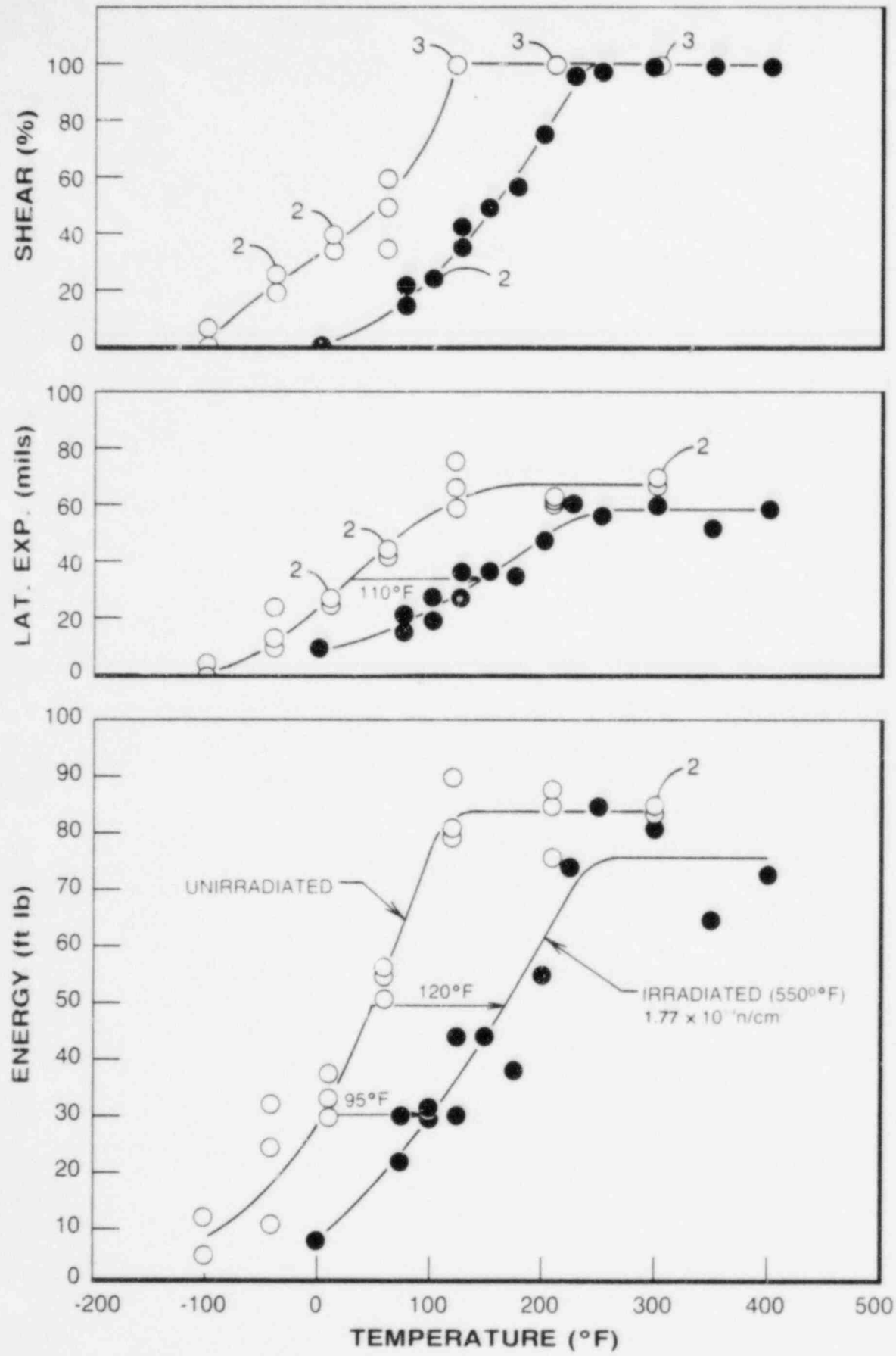

FIGURE 5-1. IRRADIATED CHARPY V-NOTCH IMPACT PROPERTIES FOR TROJAN REACTOR VESSEL LOWER SHELL PLATE C5J83-1, TRANSVERSE ORIENTATION

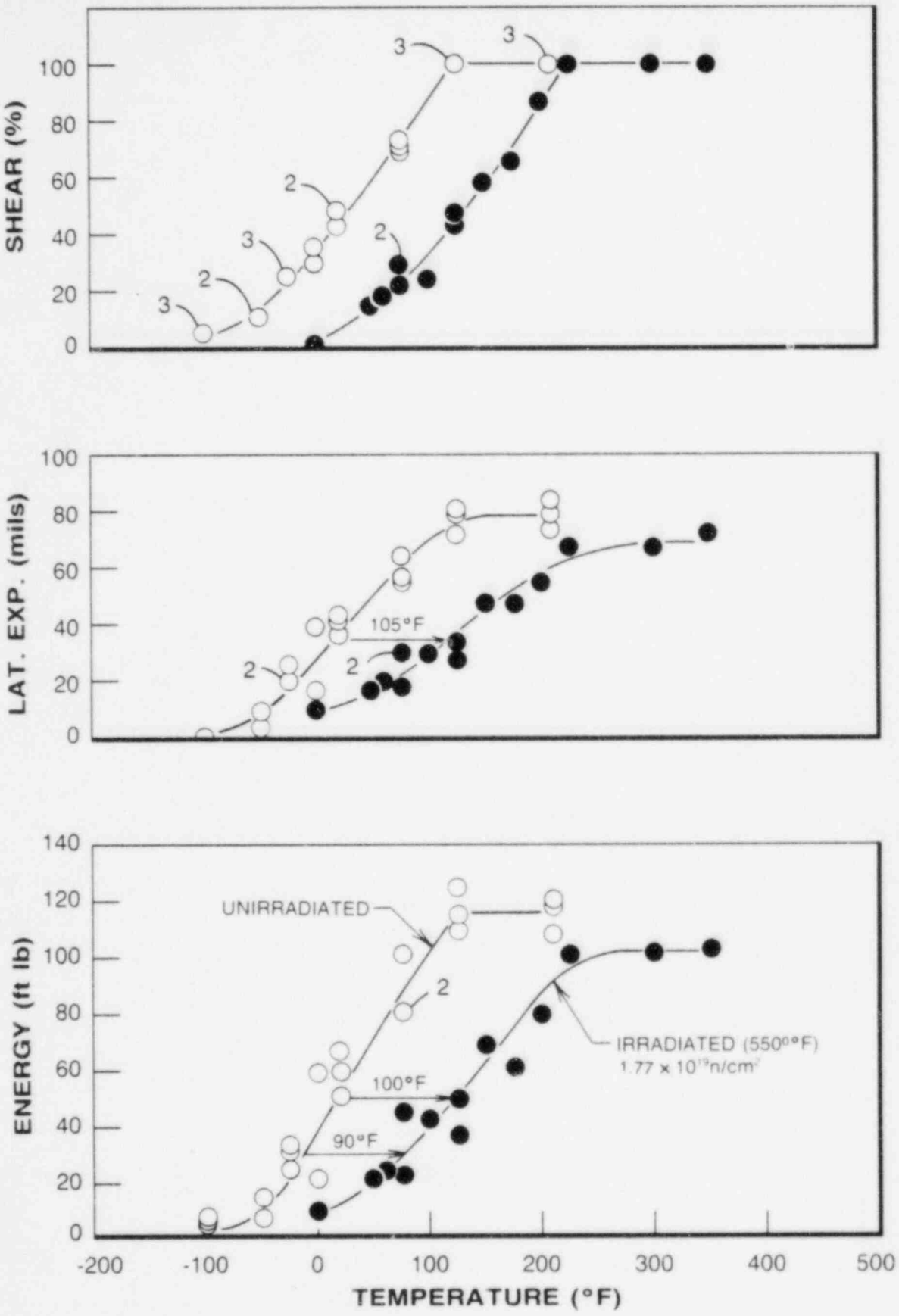

FIGURE 5-2. IRRADIATED CHARPY V-NOTCH IMPACT PROPERTIES FOR TROJAN REACTOR VESSEL LOWER SHELL PLATE C5583-1, LONGITUDINAL ORIENTATION

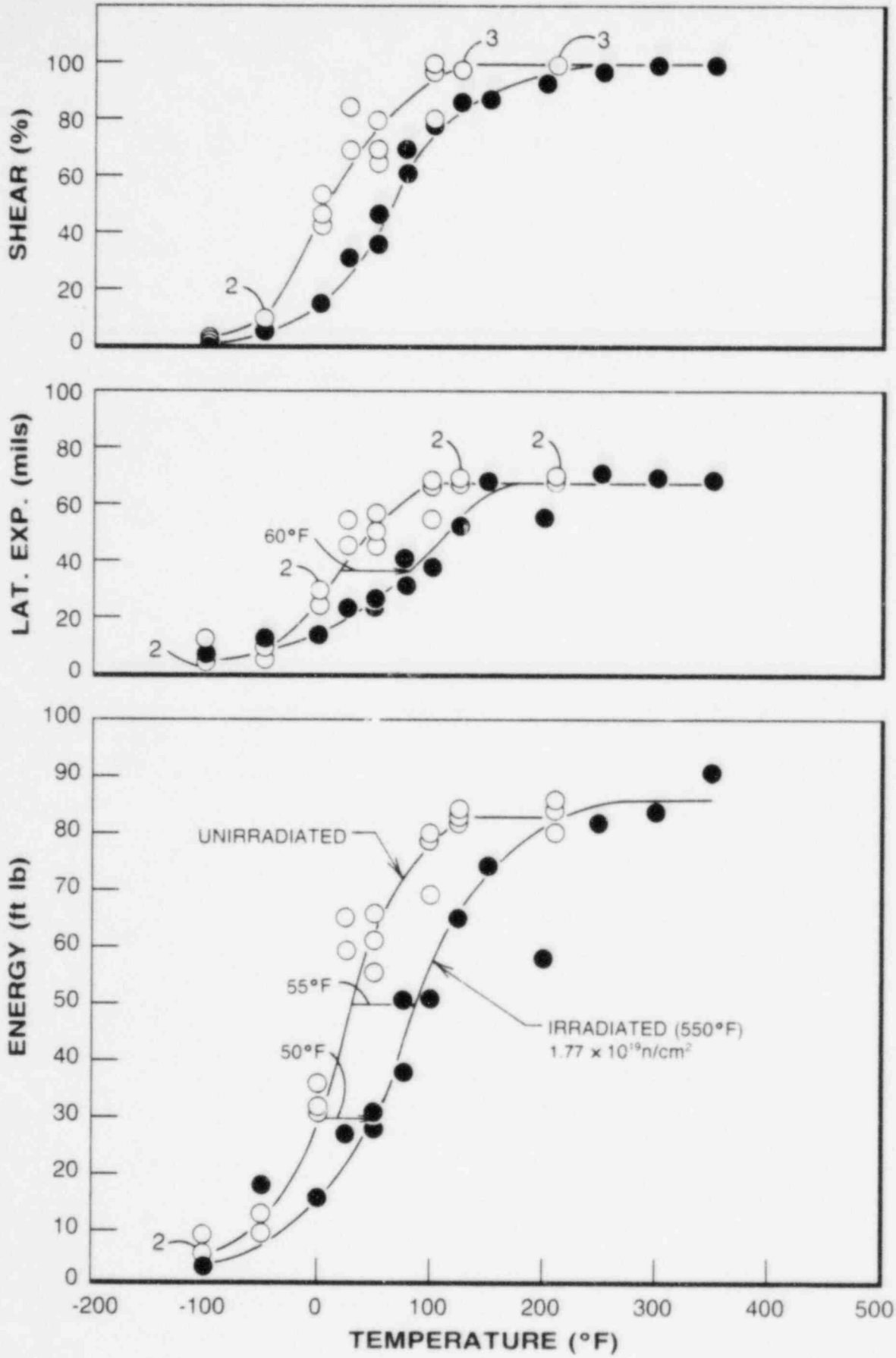

FIGURE 5-3. IRRADIATED CHARPY V-NOTCH IMPACT PROPERTIES FOR TROJAN REACTOR PRESSURE VESSEL WELD METAL

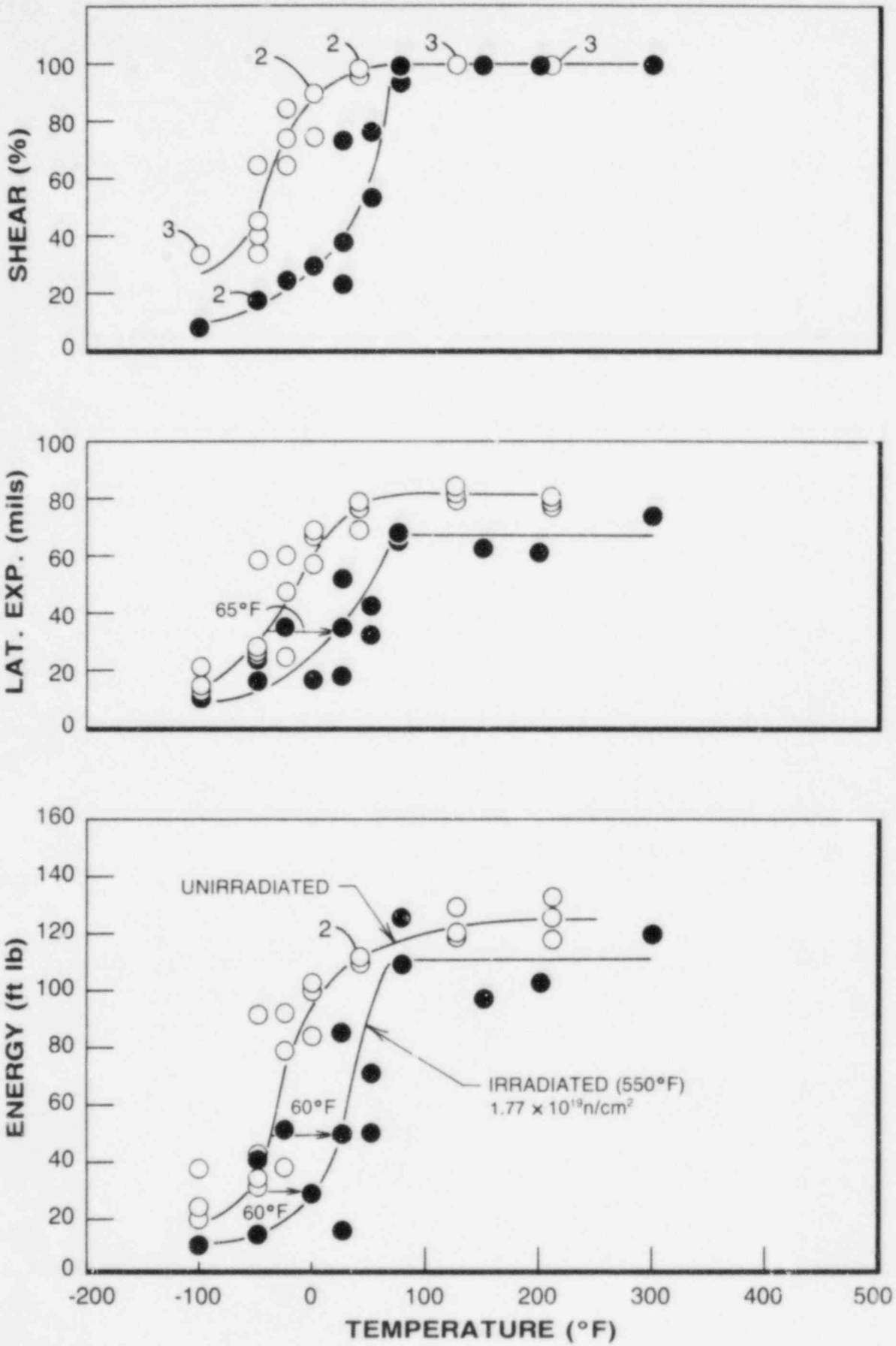

FIGURE 5-4. CHARPY V-NOTCH IMPACT PROPERTIES FOR TROJAN WELD HEAT-AFFECTED ZONE METAL

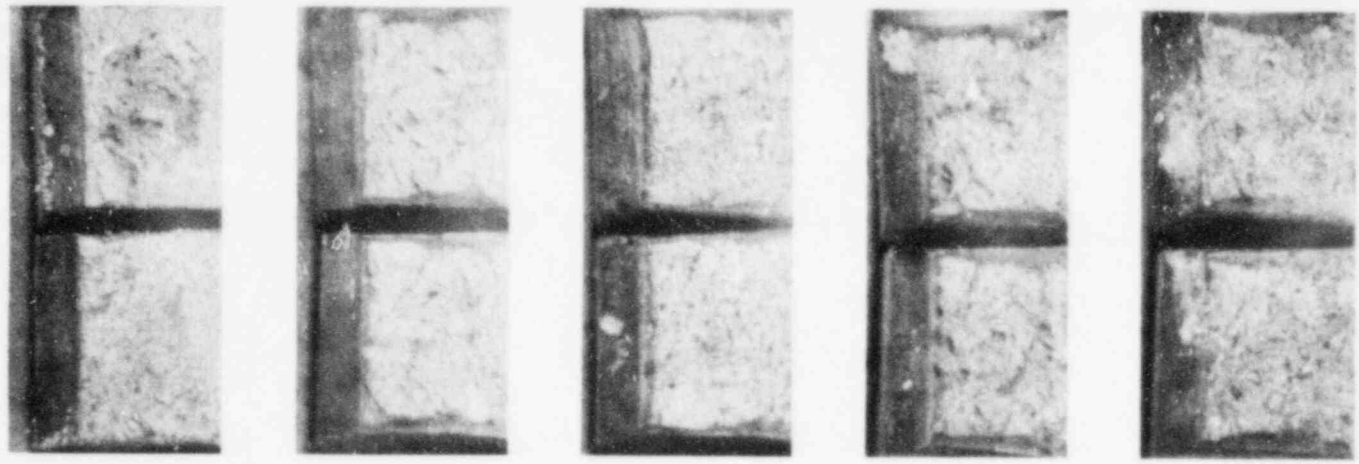

RT53 RT49 RT55 RT54 RT50

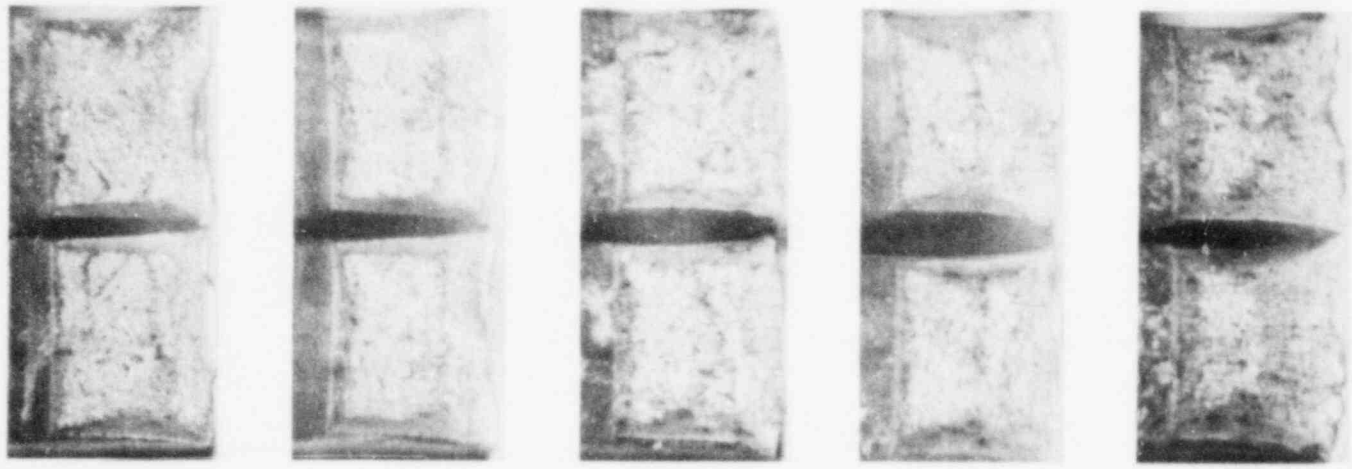

RT56 RT58 RT46 RT51 RT52

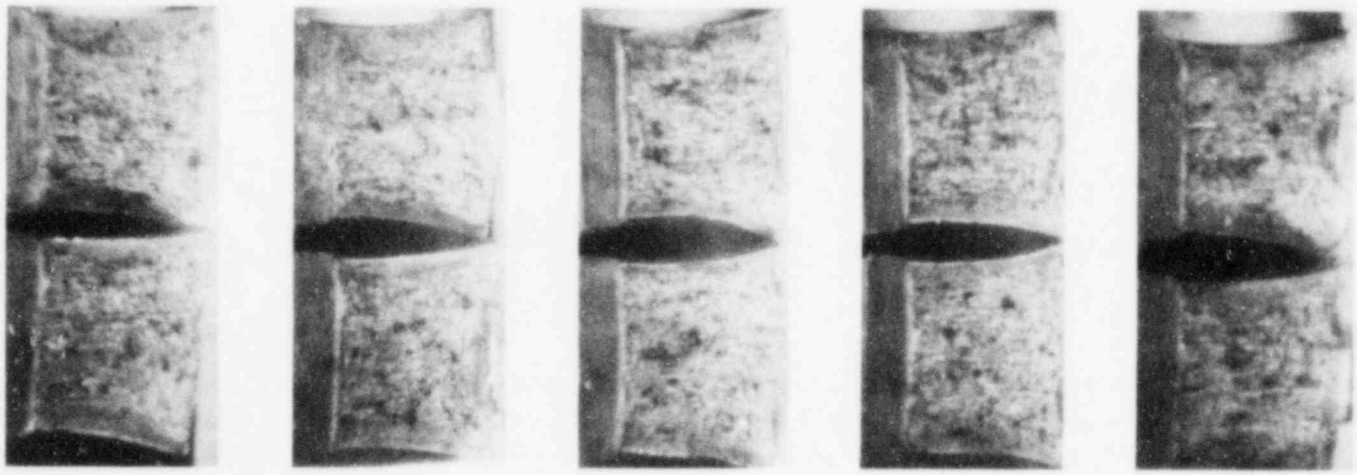

RT59 RT47 RT60 RT48 RT57

FIGURE 5-5. CHARPY IMPACT SPECIMEN FRACTURE SURFACES FOR TROJAN PRESSURE VESSEL SHELL PLATE C5583-1, TRANSVERSE ORIENTATION

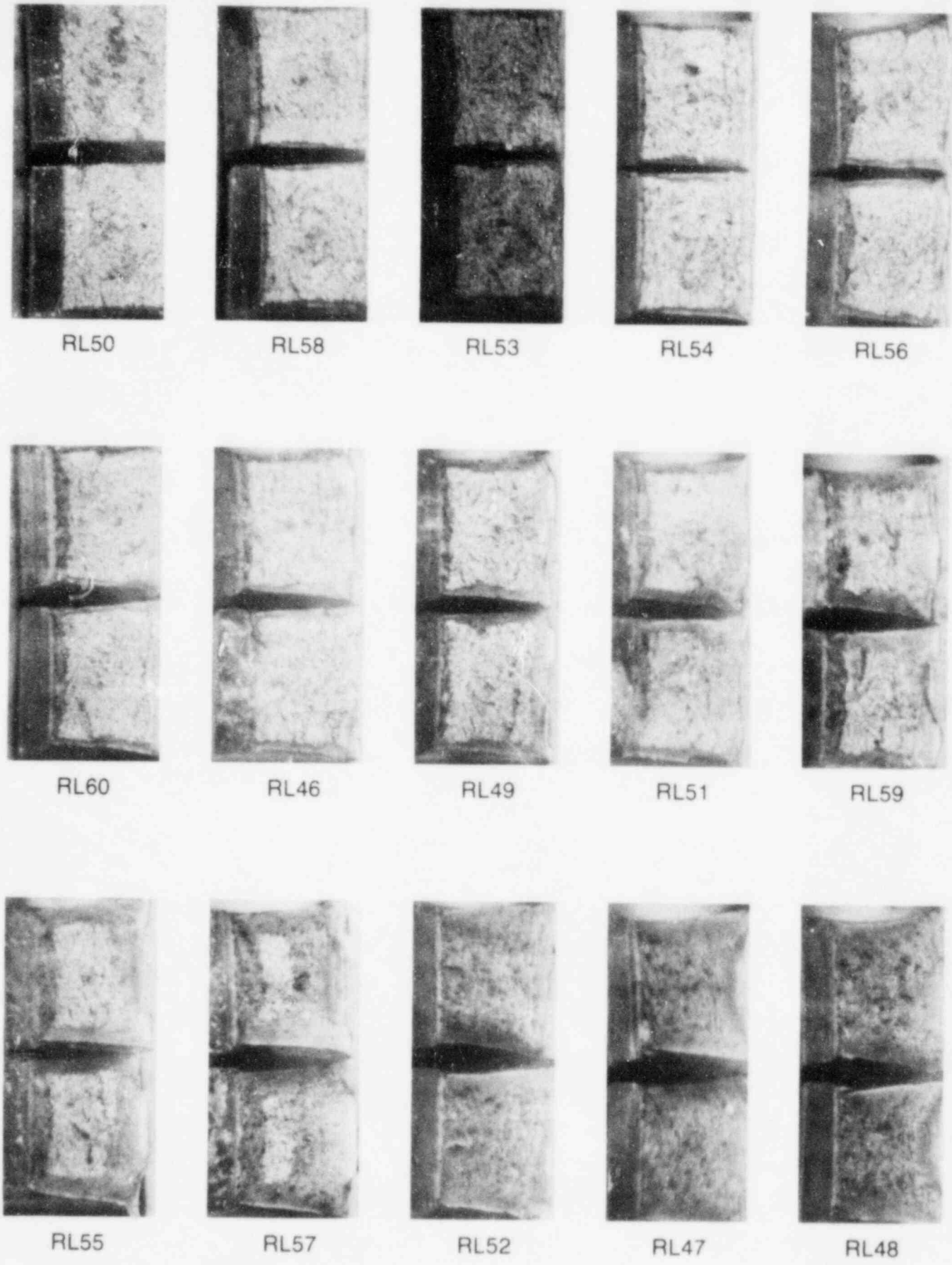

FIGURE 5-6. CHARPY IMPACT SPECIMEN FRACTURE SURFACES FOR TROJAN PRESSURE VESSEL SHELL PLATE C5583-1, LONGITUDINAL ORIENTATION

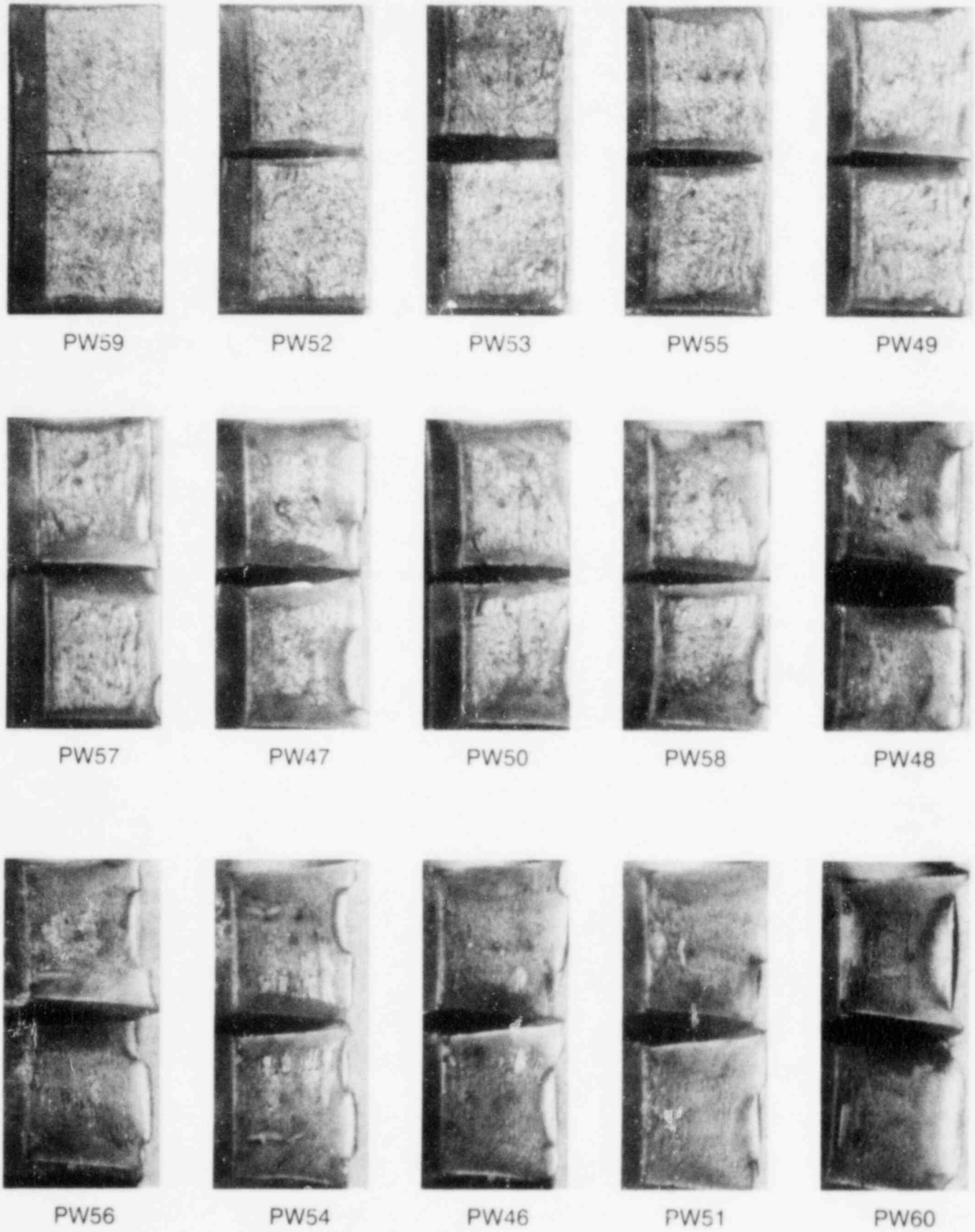

FIGURE 5-7. CHARPY IMPACT SPECIMEN FRACTURE SURFACES FOR TROJAN WELD METAL

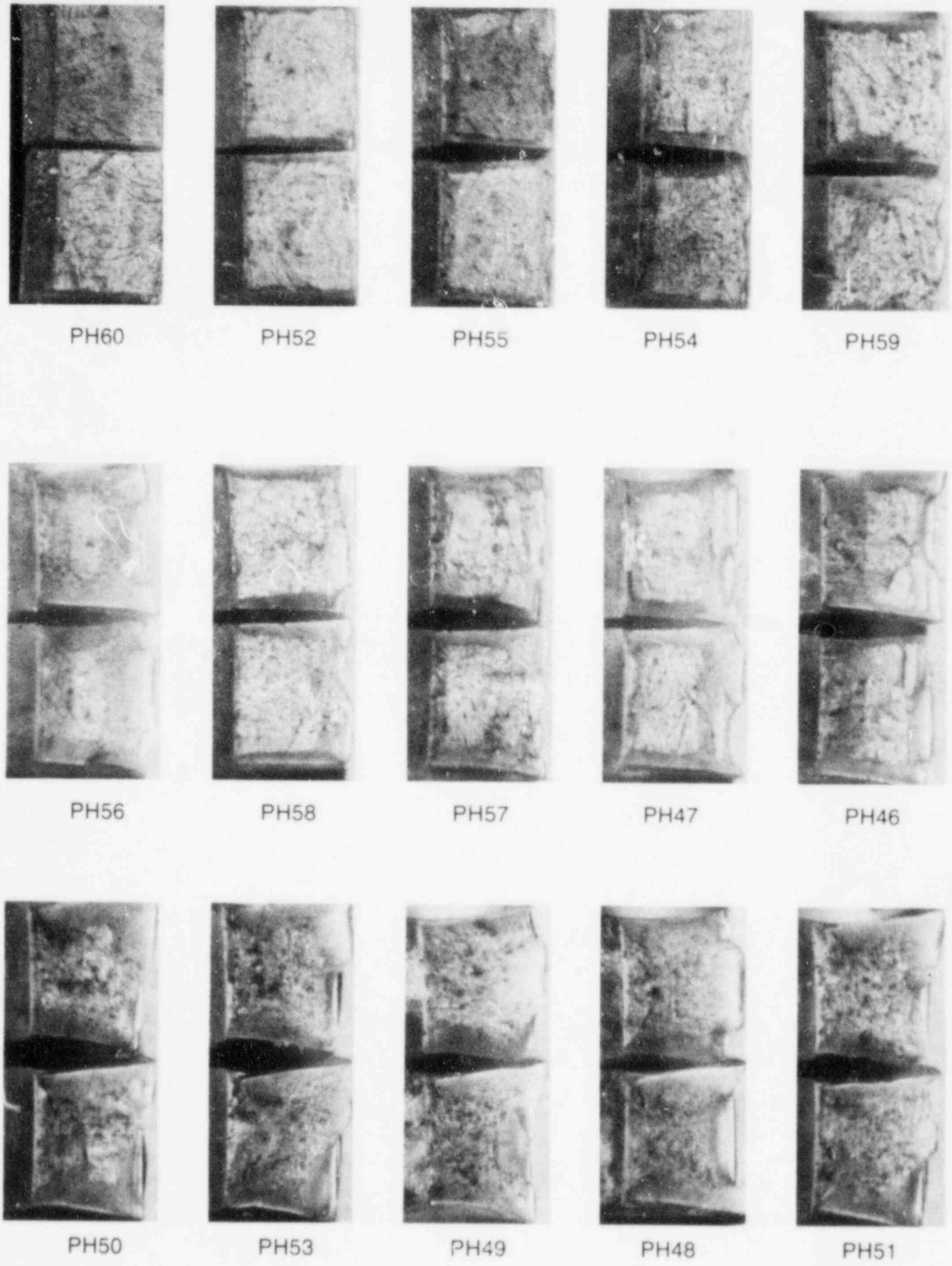

FIGURE 5-8. CHARPY IMPACT SPECIMEN FRACTURE SURFACES FOR TROJAN WELD HEAT-AFFECTED ZONE METAL

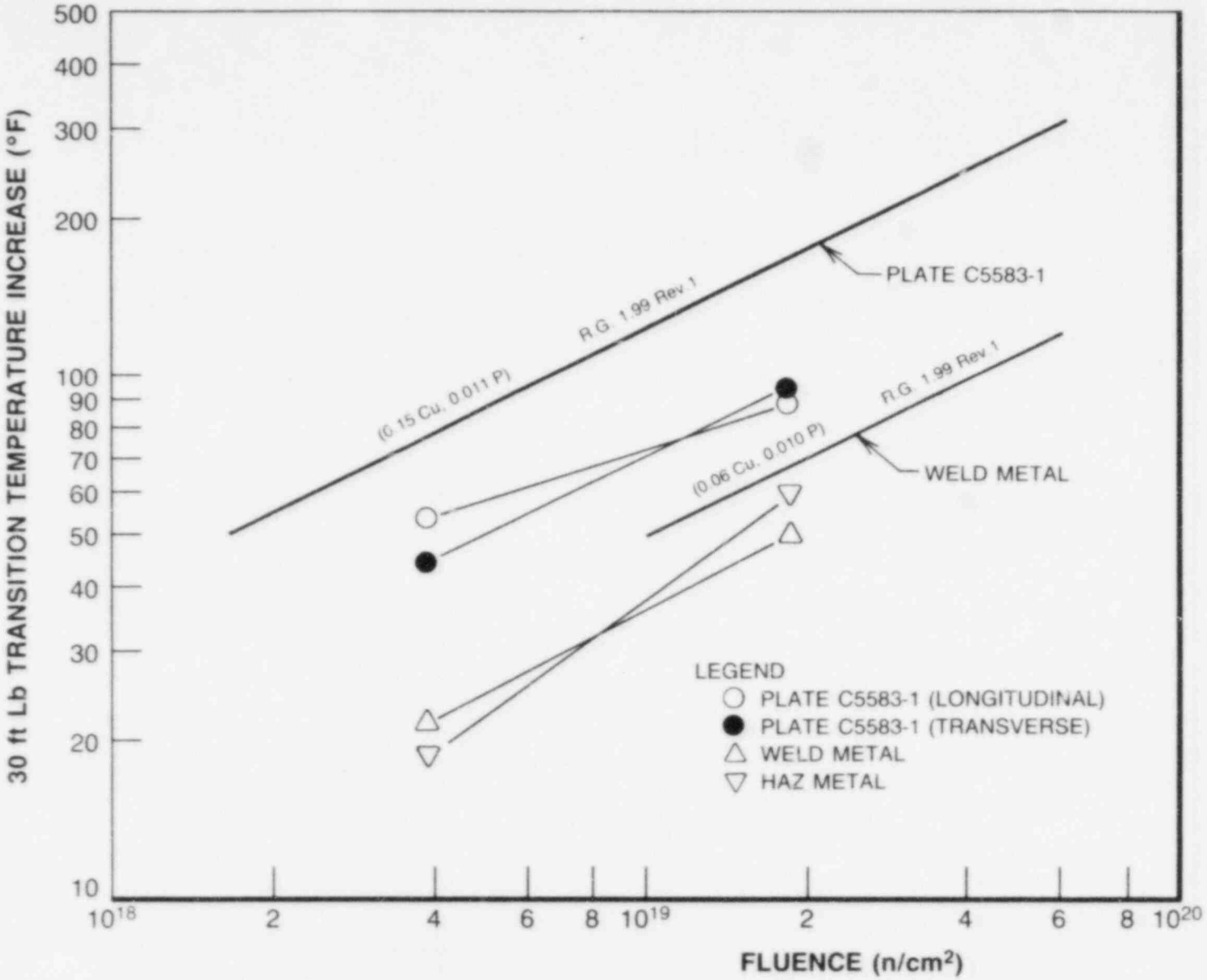

FIGURE 5-9. COMPARISON OF ACTUAL VERSUS PREDICTED 30 ft lb TRANSITION TEMPERATURE INCREASES FOR THE TROJAN REACTOR VESSEL MATERIAL BASED ON THE PREDICTION METHODS OF REGULATORY GUIDE 1.99, REVISION 1

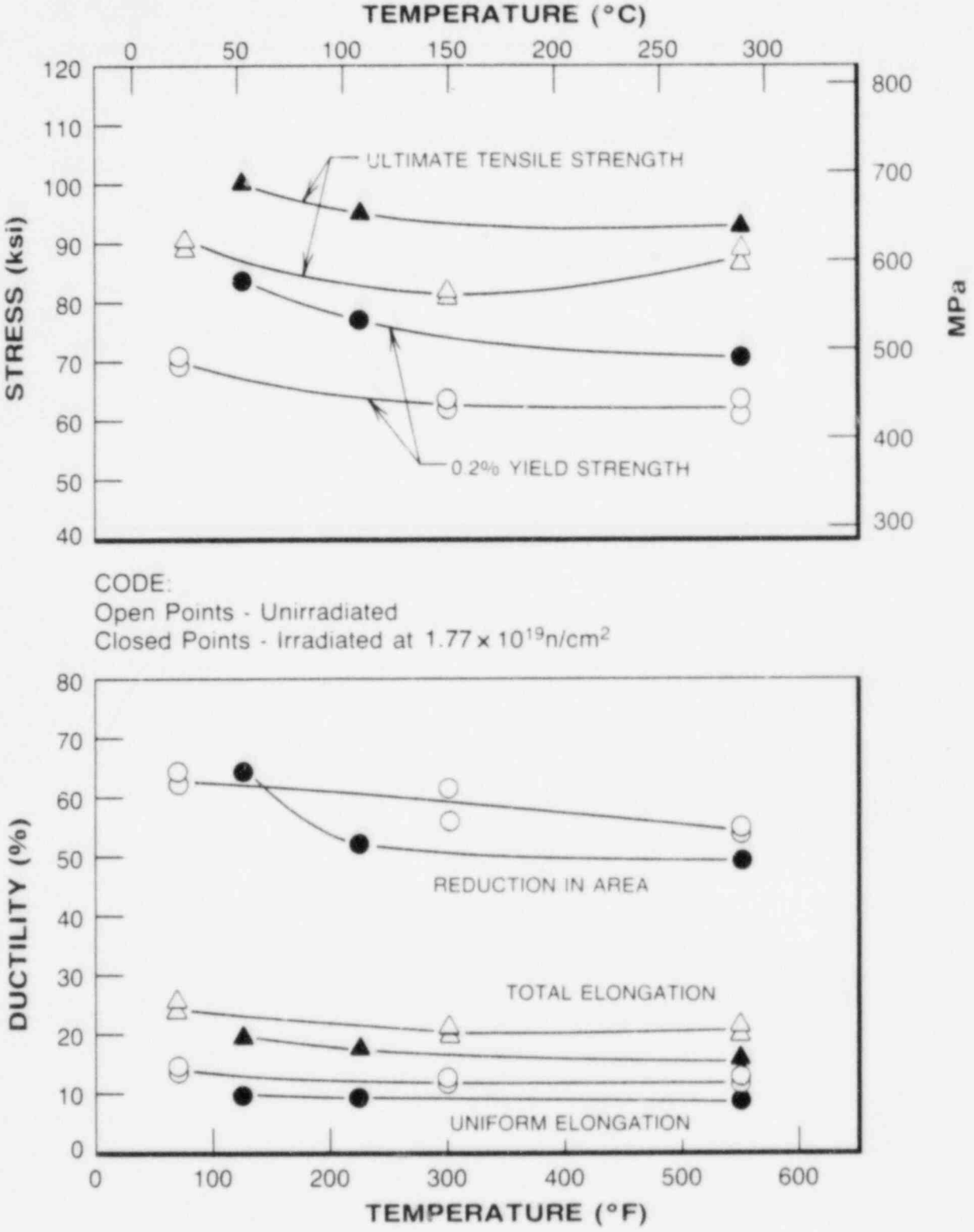

FIGURE 5-10. IRRADIATED TENSILE PROPERTIES FOR TROJAN REACTOR PRESSURE VESSEL LOWER SHELL PLATE C5583-1, TRANSVERSE ORIENTATION

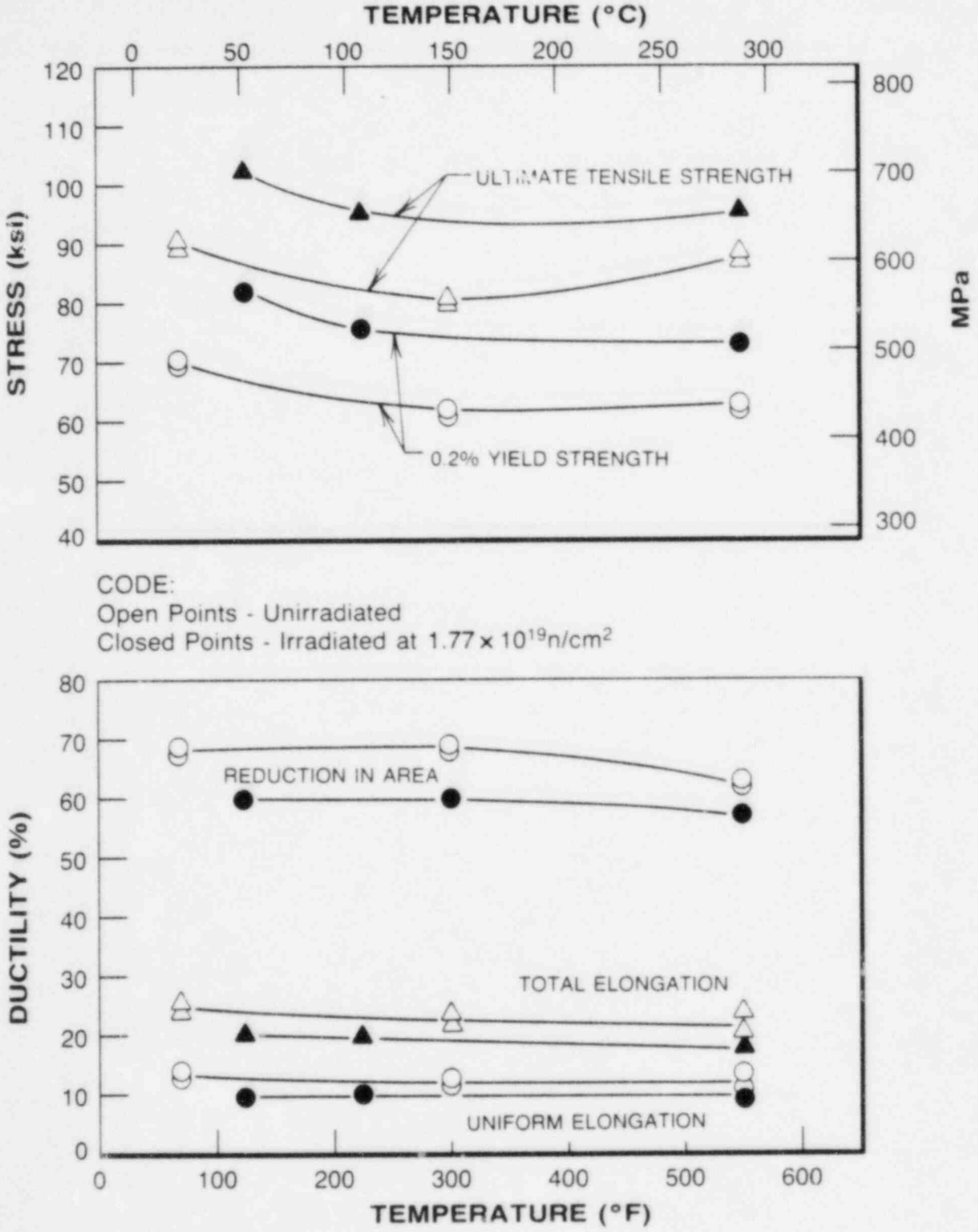

FIGURE 5-11. IRRADIATED TENSILE PROPERTIES FOR TROJAN REACTOR PRESSURE VESSEL LOWER SHELL PLATE C5583-1, LONGITUDINAL ORIENTAION

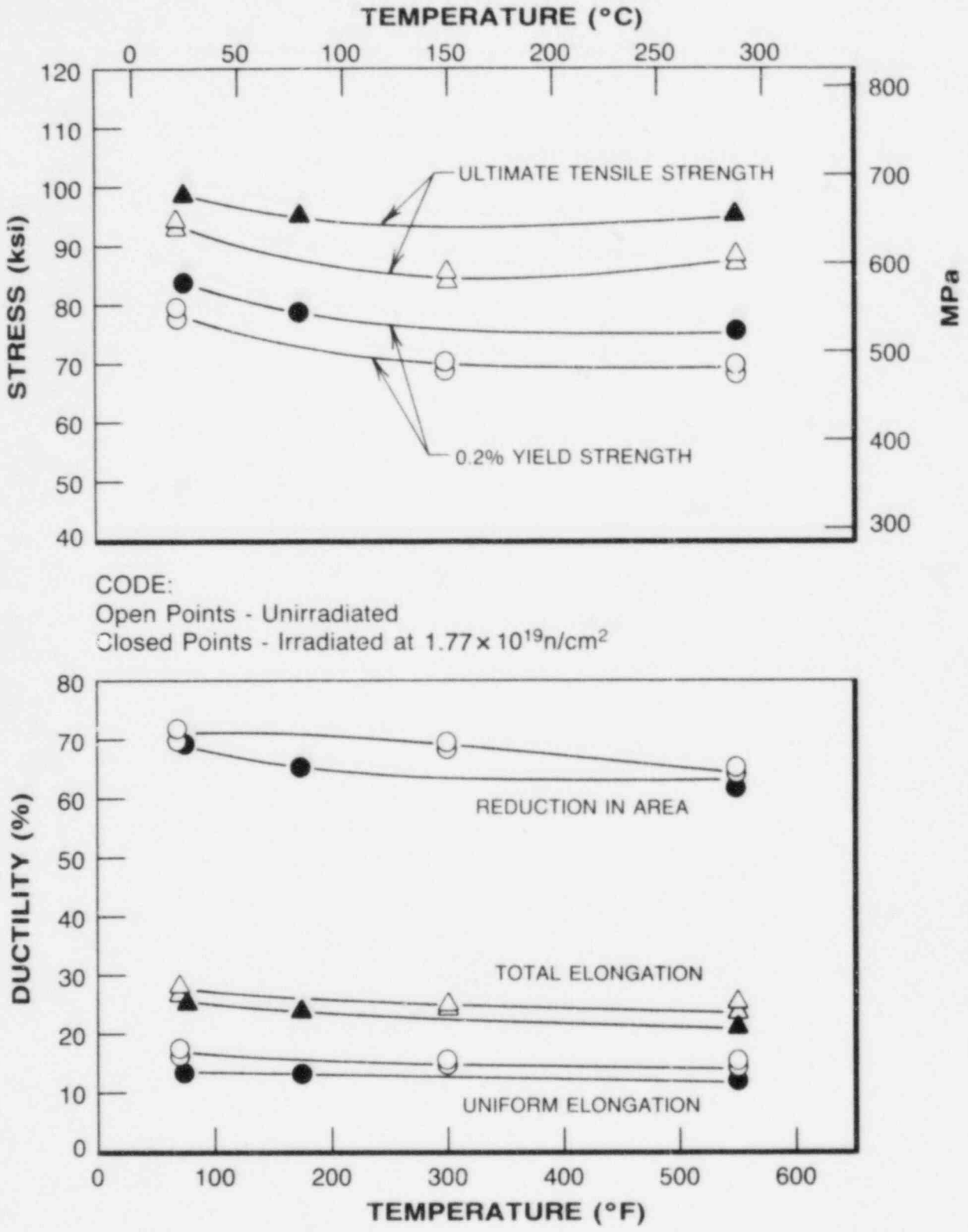

FIGURE 5-12. IRRADIATED TENSILE PROPERTIES FOR TROJAN REACTOR PRESSURE VESSEL WELD METAL

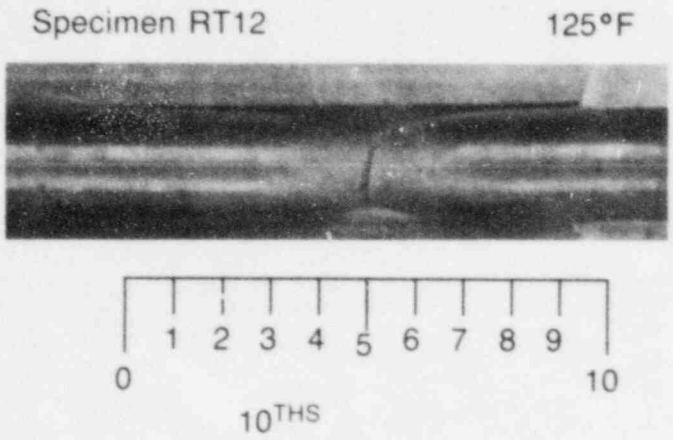

FIGURE 5-13. FRACTURED TENSILE SPECIMENS FROM TROJAN PRESSURE VESSEL LOWER SHELL PLATE C5583-1, TRANSVERSE ORIENTATION

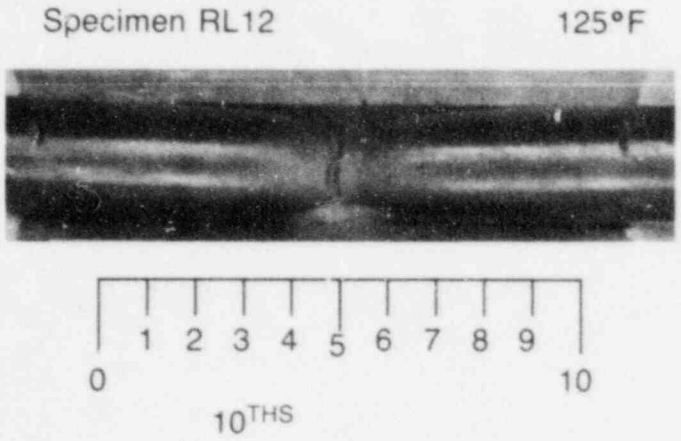

FIGURE 5-14. FRACTURED TENSILE SPECIMENS FROM TROJAN PRESSURE VESSEL LOWER SHELL PLATE C5583-1, LONGITUDINAL ORIENTATION

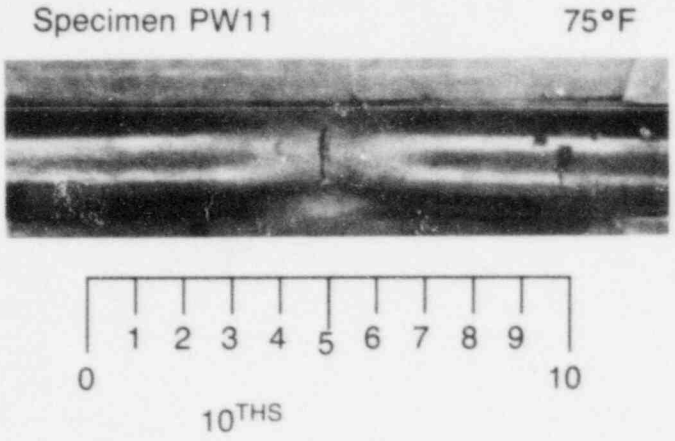

FIGURE 5-15. FRACTURED TENSILE SPECIMENS FROM TROJAN PRESSURE VESSEL WELD METAL

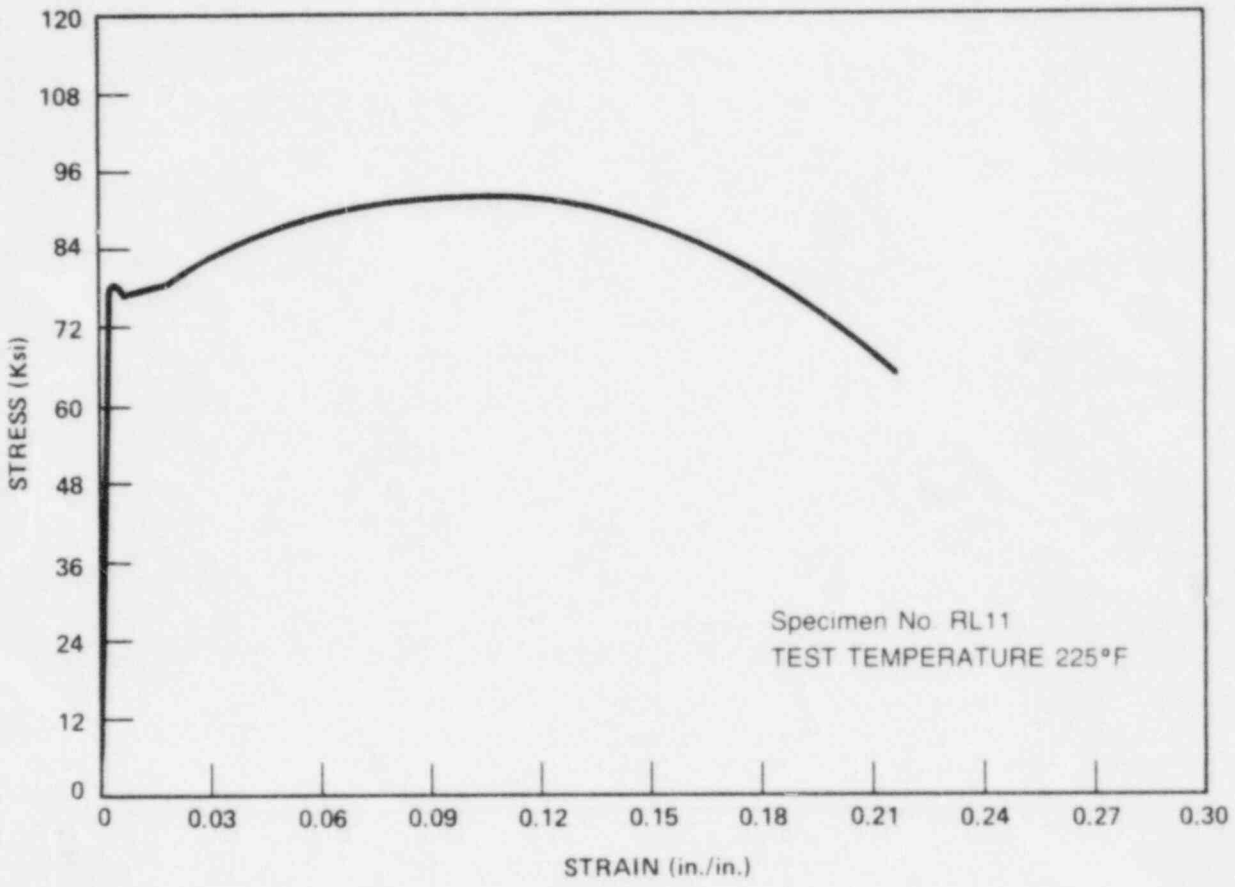

FIGURE 5-16. TYPICAL STRESS-STRAIN CURVE FOR TENSION SPECIMENS

SECTION 6
RADIATION ANALYSIS AND NEUTRON DOSIMETRY

6-1. INTRODUCTION

Knowledge of the neutron environment within the pressure vessel/surveillance capsule geometry is required as an integral part of LWR pressure vessel surveillance programs for two reasons. First, in the interpretation of radiation-induced property, changes observed in materials test specimens and the neutron environment (fluence, flux) to which the test specimens were exposed must be known. Second, in relating the changes observed in the test specimens to the present and future condition of the reactor pressure vessel, a relationship must be established between the environment at various positions within the reactor vessel and that experienced by the test specimens. The former requirement is normally met by employing a combination of rigorous analytical techniques and measurements obtained with passive neutron flux monitors contained in each of the surveillance capsules. The latter information is derived solely from analysis.

This section describes a discrete ordinates S_n transport analysis performed for the Trojan reactor to determine the fast neutron ($E > 1.0$ MeV) flux and fluence as well as the neutron energy spectra within the reactor vessel surveillance capsules. The analytical data were then used to develop lead factors for use in relating neutron exposure of the pressure vessel to that of the surveillance capsules. Based on spectrum-averaged reaction cross sections derived from this calculation, the analysis of the neutron dosimetry contained in Capsule X is presented.

6-2. DISCRETE ORDINATES ANALYSIS

A plan view of the Trojan reactor geometry at the core midplane is shown in Figure 6-1. Since the reactor exhibits $\frac{1}{8}$ core symmetry, only a zero- to 45-degree sector is depicted. Six irradiation capsules attached to the neutron pad are included in the design to constitute the reactor vessel surveillance program. Four capsules (U,W,X,Z) are located at 34 degrees and two (V,Y) at 31.5 degrees from the cardinal axes shown in Figure 6-1.

A plan view of a double surveillance capsule attached to the neutron pad is shown in Figure 6-2. The stainless steel specimen container is 1.182 inches by 1 inch and approximately 56 inches in height. The containers are positioned axially such that the specimens are centered on the core midplane, thus spanning the central 5 feet of the 12 foot high reactor core.

From a neutronic standpoint, the surveillance capsule structures are significant. In fact, they have a marked effect on the distributions of neutron flux and energy spectra in the water annulus between the neutron pad and the reactor vessel. Thus, in order to properly ascertain the neutron environment at the test specimen locations, the capsules themselves must be included in the analytical model. Use of at least a two-dimensional computation is therefore mandatory.

In the analysis of the neutron environment within the Trojan reactor geometry, predictions of neutron flux magnitude and energy spectra were made with the DOT[5] two-dimensional discrete ordinates code. The radial and azimuthal distributions were obtained from and R,θ computation wherein the geometry shown in Figures 6-1 and 6-2 was described in the analytical model. In addition to the R,θ computation, a second calculation in R,Z geometry was also carried out to obtain relative axial variations of neutron flux throughout the geometry of interest. In the R,Z analysis, the reactor core was treated as an equivalent volume cylinder and, of course, the surveillance capsules were not included in the model.

Both the R,θ and the R,Z analyses employed 47 neutron energy groups and a P_3 expansion of the scattering cross sections. The cross sections used in the analyses were obtained from the SAILOR cross section library[6] which was developed specifically for light water reactor applications. The neutron energy group structure used in the analysis is listed in Table 6-1.

A key input parameter in the analysis of the integrated fast neutron exposure of the reactor vessel is core power distribution. For this analysis, power distributions representative of time-averaged conditions derived from statistical studies of long-term operation of Westinghouse 4-loop plants were employed. These input distributions include rod-by-rod spatial variations for all peripheral fuel assemblies.

It should be noted that this generic design basis power distribution is intended to provide a vehicle for long-term (end-of-life) projection of vessel exposure. Since plant-specific

power distributions reflect only past operation, their use for projection into the future many not be justified; the use of generic data which reflects long-tem operation of similar reactor cores may provide a more suitable approach.

Benchmark testing of these generic power distributions and the SAILOR cross sections against surveillance capsule data obtained from 2-loop and 4-loop Westinghouse plants indicate that this analytical approach yields conservative results, with calculations exceeding measurements from 10 to 25 percent.[7]

One further point of interest regarding these analyses is that the design basis assumes an out-in fuel loading pattern (fresh fuel on the periphery). Future commitment to low-leakage loading patterns could significantly reduce the calculated neutron flux levels presented in Section 6-4. In addition, capsule lead factors could be changed, thereby influencing the withdrawal schedule of the remaining surveillance capsules.

Having the results of the R,θ and R,Z calculations, three-dimensional variations of neutron flux may be approximated by assuming that the following relation holds for the applicable regions of the reactor.

$$\phi(R,Z,\theta,E_g) = \phi(R,\theta,E_g) \times F(Z,E_g)$$

where:

$\phi(R,Z,\theta,E_g)$ = neutron flux at point R,Z,θ within energy group g

$\phi(R,\theta,E_g)$ = neutron flux at point R,θ within energy group g obatined from the R,θ calculation

$F(Z,E_g)$ = relative axial distribution of neutron flux within energy group g obtained from the R,Z calculation

6-3. NEUTRON DOSIMETRY

The passive neutron flux monitors included in the Trojan surveillance program are listed in Table 6-2. The first five reactions in Table 6-2 are used as fast neutron monitors to relate neutron fluence ($E > 1.0$ MeV) to measured material property changes. To properly account for burnout of the product isotope generated by fast neutron reactions,

it is necessary to also determine the magnitude of the thermal neutron flux at the monitor location. Therefore, bare and cadmium-covered cobalt-aluminum monitors were also included.

The relative locations of the various monitors within the surveillance capsules are shown in Figure 4-2. The iron, nickel, copper, and cobalt-aluminum monitors, in wire form, are placed in holes drilled in spacers at several axial levels within the capsules. The cadmium-shielded neptunium and uranium fission monitors are are accomodated within the dosimeter block located near the center of the capsule.

The use of passive monitors such as those listed in Table 6-2 does not yield a direct measure of the energy-dependent flux level at the point of interest. Rather, the activation or fission process is a measure of the integrated effect that the time- and energy-dependent neutron flux has on the target material over the course of the irradiation period. An accurate assessment of the average neutron flux level incident on the various monitors may be derived from the activation measurements only if the irradiation parameters are well known. In particular, the following variables are of interest:

- The operating history of the reactor
- The energy response of the monitor
- The neutron energy spectrum at the monitor location
- The physical characteristics of the monitor

The analysis of the passive monitors and subsequent derivation of the average neutron flux requires completion of two operations. First, the disintegration rate of product isotope per unit mass of monitor must be determined. Second, in order to define a suitable spectrum-averaged reaction cross section, the neutron energy spectrum at the monitor location must be calculated.

The specific activity of each of the monitors is determined using established ASTM procedures.[8,9,10,11,12] Following sample preparation, the activity of each monitor is determined by means of a lithium-drifted germanium, Ge(Li), gamma spectrometer. The overall standard deviation of the measured data is a function of the precision of sample weighing, the uncertainty in counting, and the acceptable error in detector calibration.

For the samples removed from Trojan, the overall 2σ deviation in the measured data is determined to be plus or minus 10 percent. The neutron energy spectra are determined analytically using the method described in paragraph 6-1.

Having the measured activity of the monitors and the neutron energy spectra at the locations of interest, the calculation of the neutron flux proceeds as follows. The reaction product activity in the monitor is expressed as:

$$R = \frac{N_O}{A} f_i Y \int_E \sigma(E)\, \phi(E) dE \sum_{j=1}^{N} \frac{P_j}{P_{max}} (1 - e^{-\lambda t_j})\, e^{-\lambda t_d} \qquad (6\text{-}2)$$

where:

R = induced product activity

N_O = Avagadro's number

A = atomic weight of the target isotope

f_i = weight fraction of the target isotope in the target material

Y = number of product atoms produced per reaction

$\sigma(E)$ = energy dependent reaction cross section

$\phi(E)$ = energy dependent neutron flux at the monitor location with the reactor at full power

P_j = average core power level during irradiation period j

P_{max} = maximum or reference core power level

λ = decay constant of the product isotope

t_j = length of irradiation period j

t_d = decay time following irradiation period j

Because neutron flux distributions are calculated using multigroup transport methods and, further, because the prime interest is in the fast neutron flux above 1.0 MeV, spectrum-averaged reaction cross sections are defined such that the integral term in equation (6-2) is replaced by the following relation.

$$\int_E \sigma(E)\,\phi(E)dE = \bar{\sigma}\,\phi(E > 1.0\ \text{MeV})$$

where:

$$\bar{\sigma} = \frac{\int_0^\infty \sigma(E)\,\phi(E)dE}{\int_{1.0\ \text{MeV}}^\infty \phi(E)dE} = \frac{\sum_{G=1}^{N} \sigma_g \phi_g}{\sum_{G=G_{1.0\ \text{MeV}}}^{N} \phi_g}$$

Thus, equation (6-2) is rewritten

$$R = \frac{N_O}{A} f_i\, Y\, \bar{\sigma}\, \phi\,(E > 1.0\ \text{MeV}) \sum_{j=1}^{N} \frac{P_j}{P_{max}} (1 - e^{-\lambda t_j})\, e^{-\lambda t_d}$$

or solving for the neutron flux,

$$\phi\,(E > 1.0\ \text{MeV}) = \frac{R}{\frac{N_O}{A} f_i\, Y\, \bar{\sigma} \sum_{j=1}^{N} \frac{P_j}{P_{max}} (1 - e^{-\lambda t_j})\, e^{-\lambda t_d}} \qquad (6\text{-}3)$$

The total fluence above 1.0 MeV is then given by

$$\bar{\Phi}\,(E > 1.0\ \text{MeV}) = \Phi\,(E > 1.0\ \text{MeV}) \sum_{j=1}^{N} \frac{P_j}{P_{max}} t_j \qquad (6\text{-}4)$$

where:

$\sum_{j=1}^{N} \frac{P_j}{P_{max}} t_j$ = total effective full power seconds of reactor operation up to the time of capsule removal

An assessment of the thermal neutron flux levels within the surveillance capsules is obtained from the bare and cadmium-covered Co^{59} (n,γ) Co^{60} data by means of cadmium ratios and the use of a 24-barn temperature corrected 2200 m/sec cross section. Thus,

$$\Phi_{Th} = \frac{R_{bare}\left[\frac{D-1}{D}\right]}{\frac{N_O}{A} f_i Y \bar{\sigma} \sum_{j=1}^{N} \frac{P_j}{P_{max}} (1 - e^{-\lambda t_j}) e^{-\lambda t_d}} \quad (6\text{-}5)$$

where:

D is defined as $\frac{R_{bare}}{R_{Cd\ covered}}$

6-4. TRANSPORT ANALYSIS RESULTS

Results of the S_n transport calculations for Trojan reactor are summarized in Figures 6-3 through 6-6 and in Tables 6-3 through 6-5. In Figure 6-3, the calculated maximum neutron flux levels at the surveillance capsule centerline, pressure vessel inner radius, ¼ thickness location, and ¾ thickness location are presented as a function of azimuthal angle. The influence of the surveillance capsules on the fast neutron flux distribution is clearly evident. In Figure 6-4, the radial distribution of maximum fast neutron flux (E > 1.0 MeV) through the thickness of the reactor pressure vessel is shown. The relative axial variation of neutron flux within the vessel is given in Figure 6-5. Absolute axial variations of fast neutron flux may be obtained by multiplying the levels given in Figure 6-3 or 6-4 by the appropriate values from Figure 6-5.

In Figure 6-6, the radial variations of fast neutron flux within the surveillance capsules are presented. These data, in conjunction with the maximum vessel flux, are used to develop lead factors for each of the capsules. Here the lead factor is defined as the ratio of the fast neutron flux (E > 1.0 MeV) at the dosimeter block location (capsule center)

to the maximum fast neutron flux at the pressure vessel inner radius. The updated lead factors for the Trojan surveillance capsules are listed in Table 6-3. The neutron flux monitors contained within the surveillace capsule are all located at the same radial location, the capsule center. Had they been located at different radial locations within the capsules it would have been necessary to adjust the disintegration rates for the gradients that exist within the capsules. In the present analysis, the point of comparison for all reaction rates is, of course, the capsule center.

In order to derive neutron flux and fluence levels from the measured disintegration rates, suitable spectrum-averaged reaction cross sections are required. The neutron energy spectrum calculated to exist at the center of the Trojan surveillance Capsule X is listed in Table 6-4. The associated spectrum-averaged cross sections for each of the fast neutron reactions are given in Table 6-5.

6-5. DOSIMETRY RESULTS

The irradiation history of the Trojan reactor up to the time of removal of Capsule X is listed in Table 6-6. Comparisons of measured and calculated saturated activity of the flux monitors contained in Capsule X based on the irradiation history shown in Table 6-6 are listed in Table 6-7. The data are presented as measured at the capsule center.

The fast neutron ($E > 1.0$ MeV) flux and fluence levels derived for Capsule X are presented in Table 6-8. The thermal neutron flux obtained from the cobalt-aluminum monitors is summarized in Table 6-9. Due to the relatively low thermal neutron flux at the capsule location, no burnup correction was made to any of the measured activities. The maximum error introduced by this assumption is estimated to be less than 1 percent for the Ni^{58} (n,p)Co^{58} reaction and even less significant for all of the other fast neutron reactions.

An examination of Table 6-8 shows that the fast neutron flux ($E > 1.0$ MeV) derived from the five threshold reactions ranges from 1.14×10^{11} to 1.61×10^{11} n/cm^2-sec, a total span of about 41 percent. It may also be noted that the calculated flux value of 1.36×10^{11}n/cm^2-sec compares well with the average measured value of 1.31×10^{11} n/cm^2-sec with individual calculation to experimental ratios ranging from 0.84 to 1.19.

Comparisons of measured and calculated fast neutron exposures for Capsule X and the inner radius of the pressure vessel are presented in Table 6-10. Calculated current and EOL vessel exposures are presented in Table 6-11, for vessel inner radius, ¼ thickness and ¾ thickness. Agreement of 4% between the average measured value and the calculation supports the use of the calculated exposure for vessel embrittlement projections. Based on the data given in Table 6-10, the best estimate exposure of Capsule X is 1.77×10^{19} n/cm^2 ($E > 1.0$ MeV).

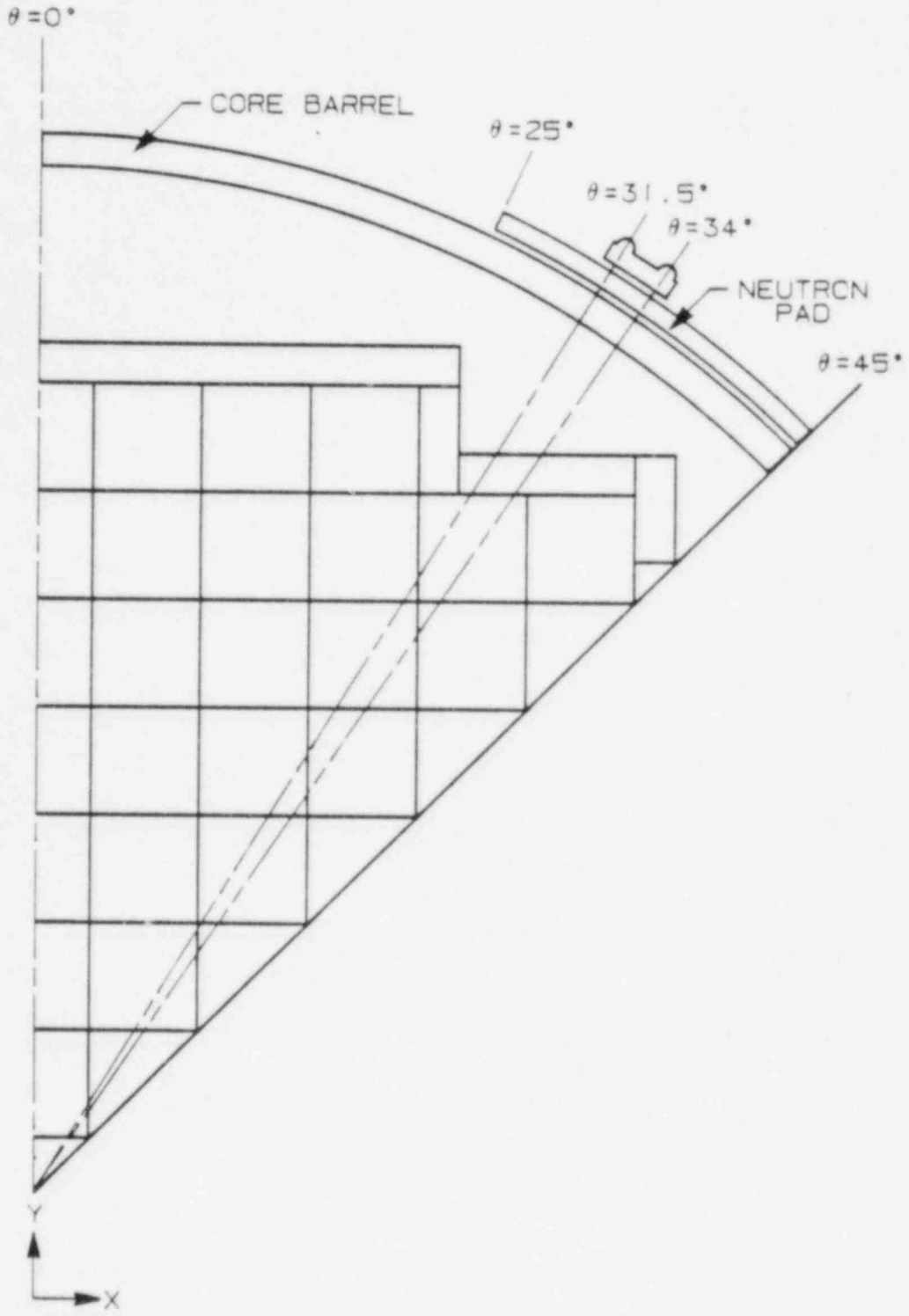

FIGURE 6-1. TROJAN REACTOR GEOMETRY

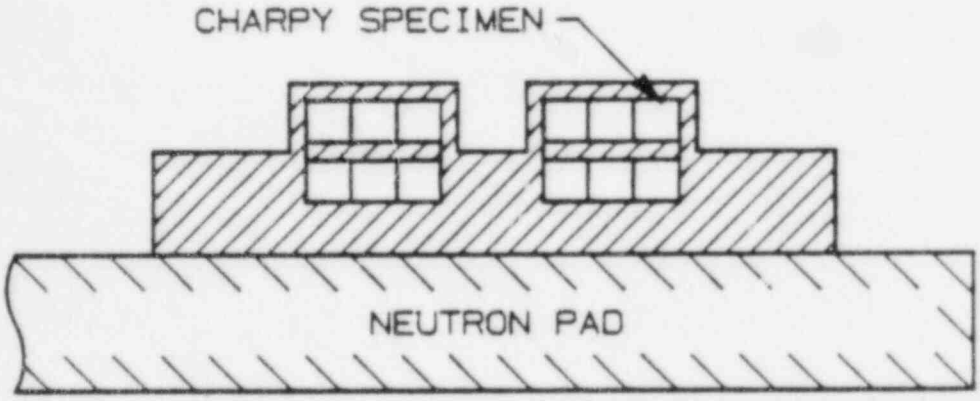

FIGURE 6-2. PLAN VIEW OF A REACTOR VESSEL SURVEILLANCE CAPSULE

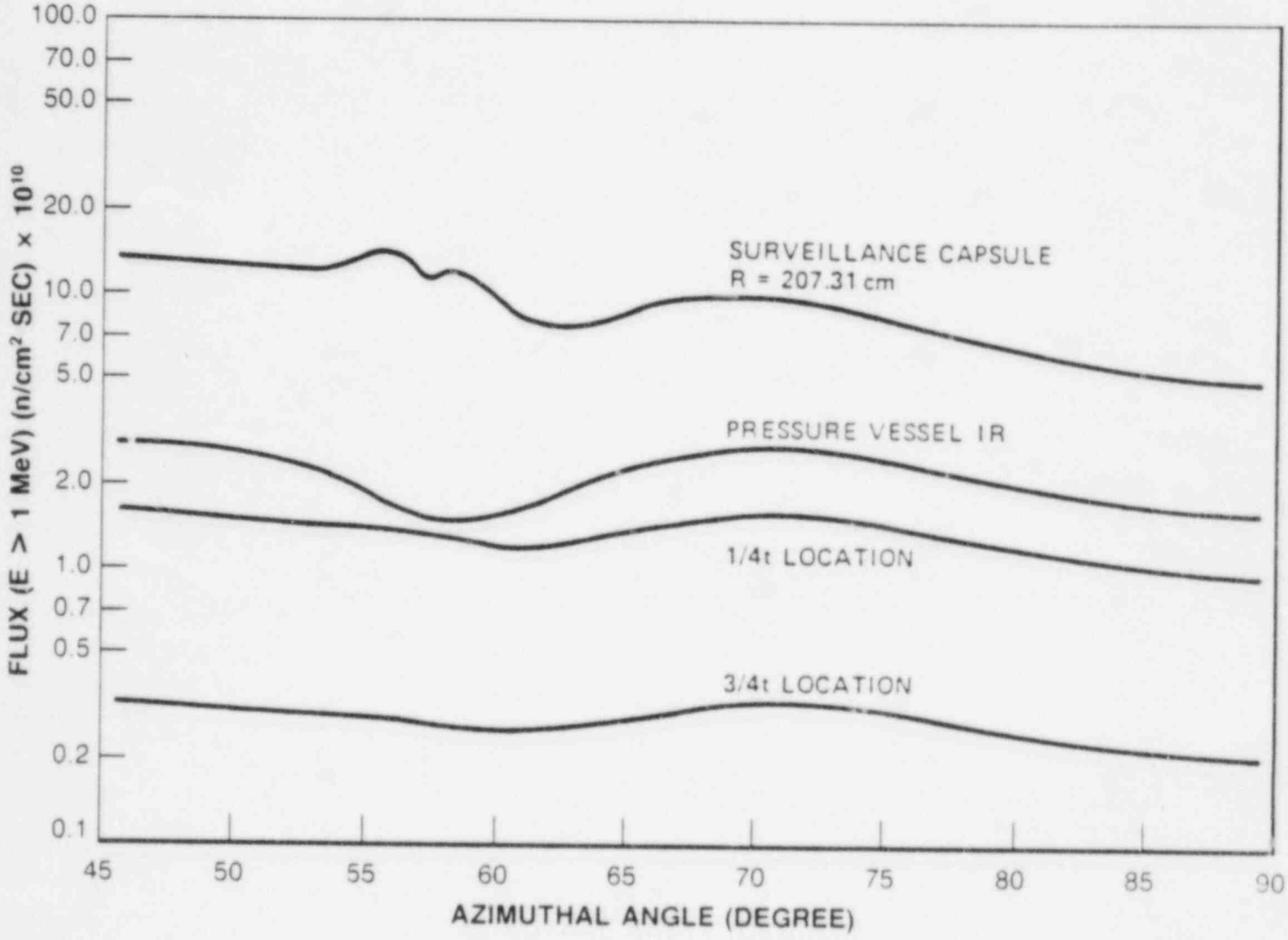

FIGURE 6-3. CALCULATED AZIMUTHAL DISTRIBUTION OF MAXIMUM FAST NEUTRON FLUX (E > 1.0 MeV) WITHIN THE PRESSURE VESSEL — SURVEILLANCE CAPSULE GEOMETRY

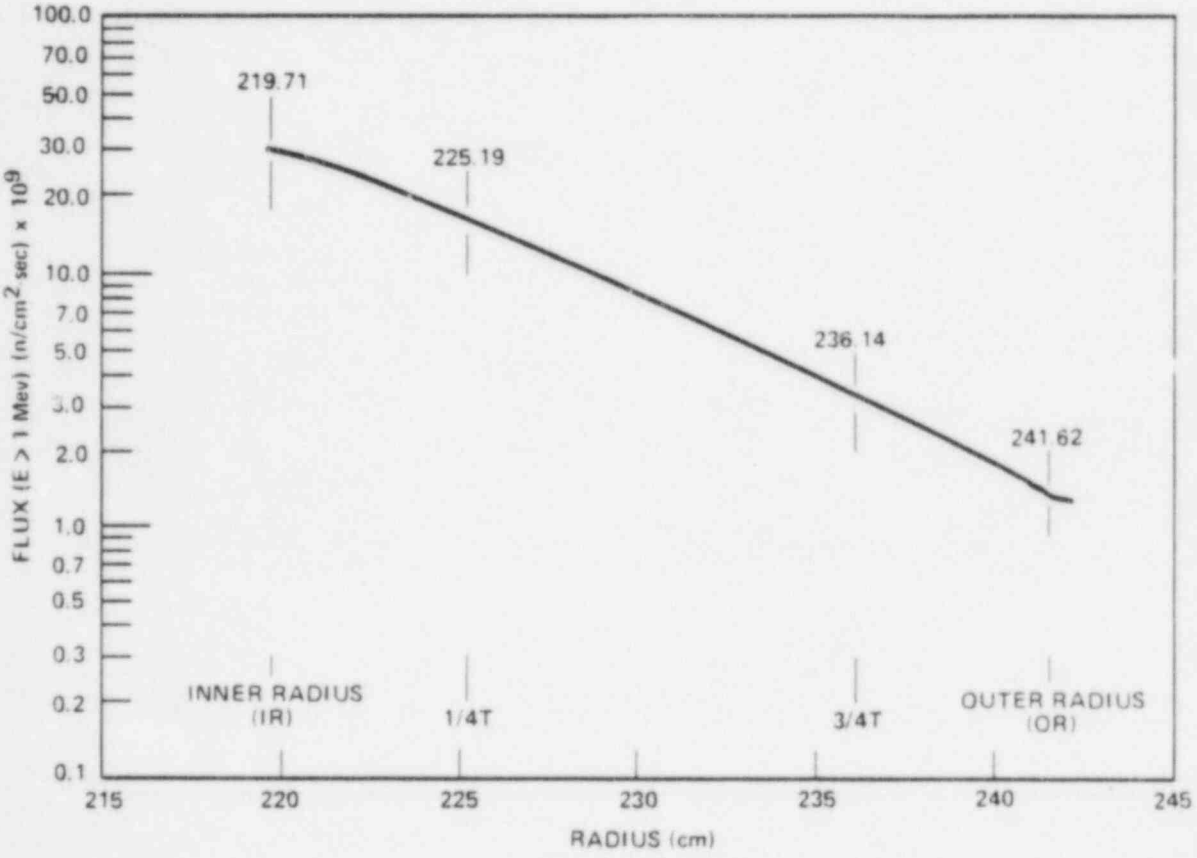

FIGURE 6-4. CALCULATED RADIAL DISTRIBUTION OF MAXIMUM FAST NEUTRON FLUX (E > 1.0 MeV) WITHIN THE PRESSURE VESSEL

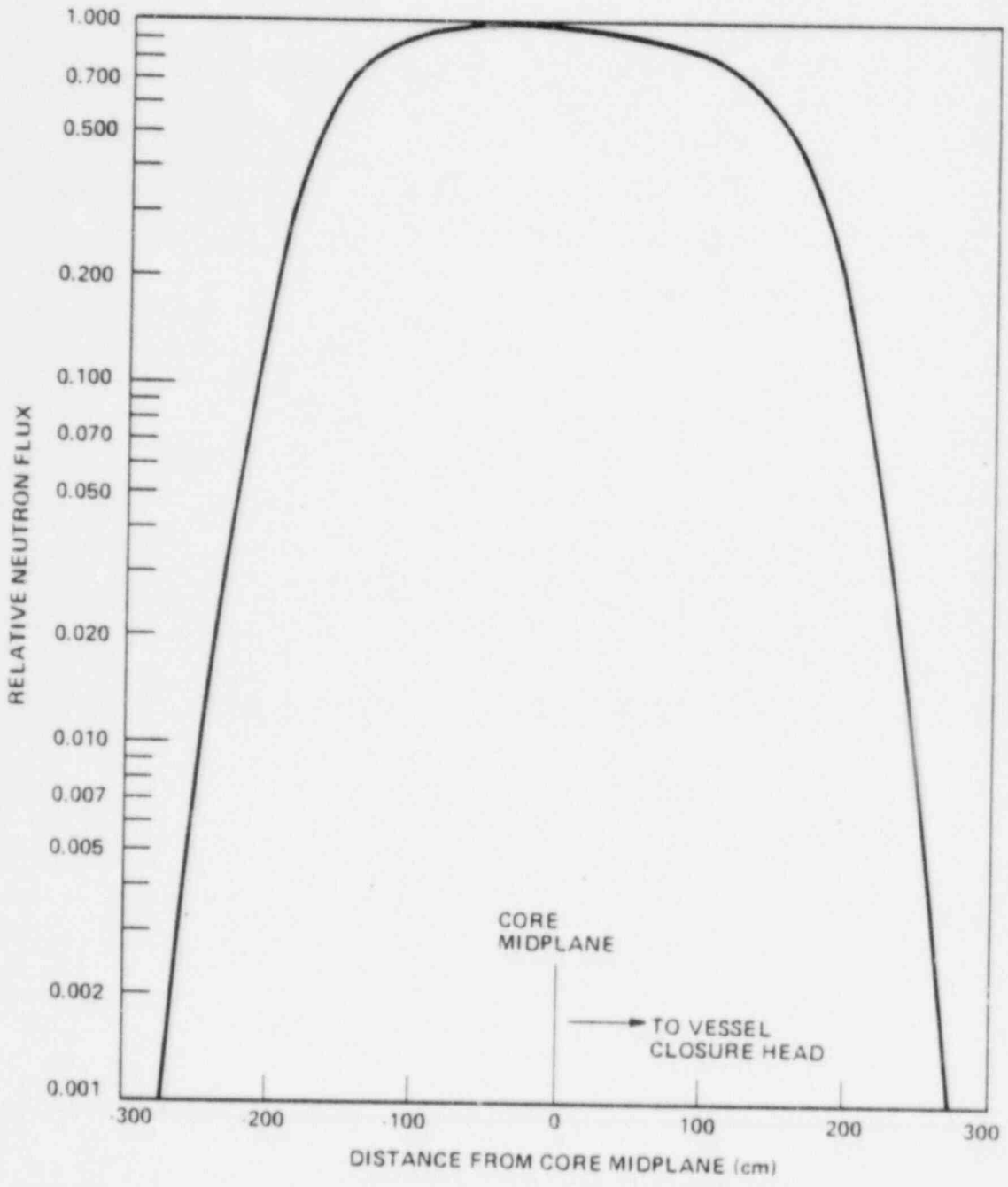

FIGURE 6-5. RELATIVE AXIAL VARIATION OF FAST NEUTRON FLUX ($E > 1.0$ MeV) WITHIN THE PRESSURE VESSEL

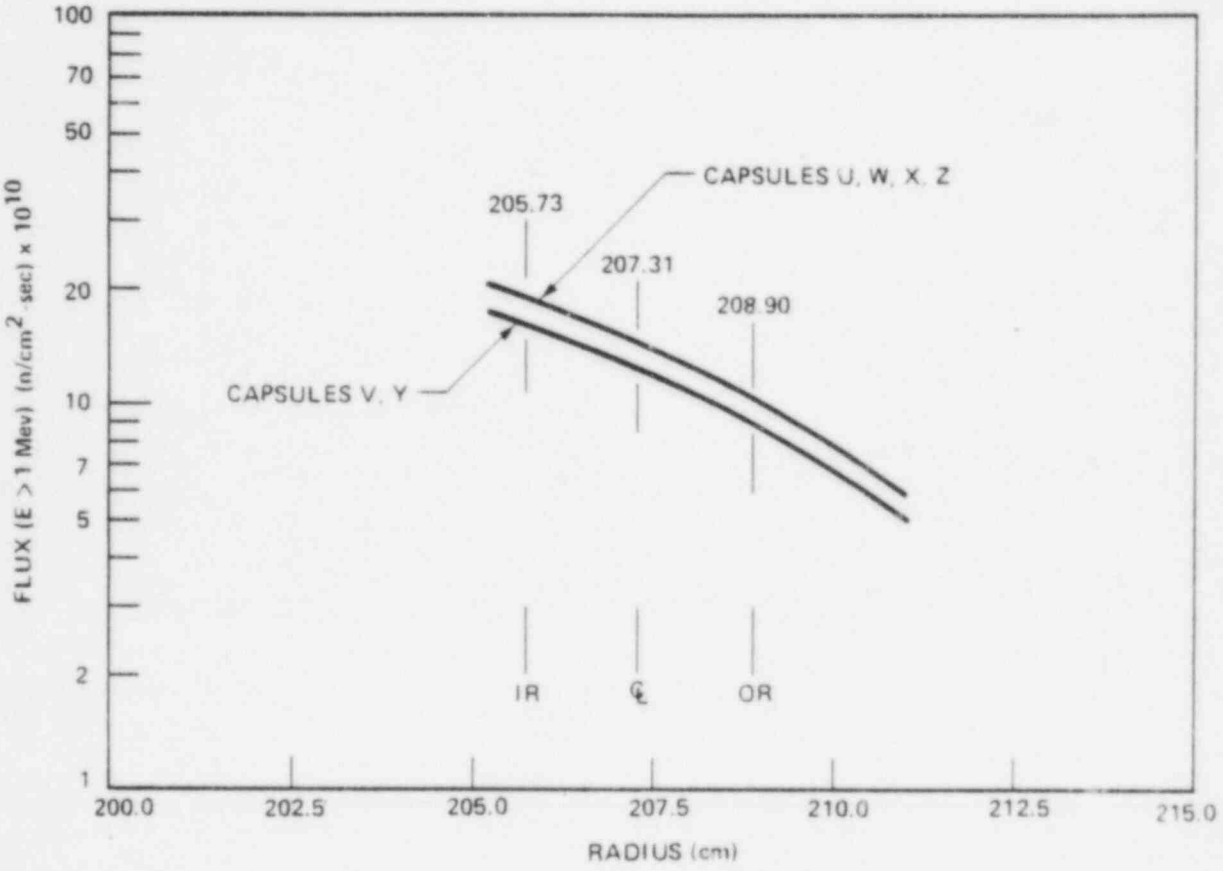

FIGURE 6-6. CALCULATED RADIAL DISTRIBUTION OF MAXIMUM FAST NEUTRON FLUX (E > 1.0 MeV) WITHIN THE SURVEILLANCE CAPSULES

TABLE 6-1
47 GROUP ENERGY STRUCTURE

Group	Lower Energy (MeV)	Group	Lower Energy (MeV)
1	14.19[a]	25	0.183
2	12.21	26	0.111
3	10.00	27	0.0674
4	8.61	28	0.0409
5	7.41	29	0.0318
6	6.07	30	0.0261
7	4.97	31	0.0242
8	3.68	32	0.0219
9	3.01	33	0.0150
10	2.73	34	7.10×10^{-3}
11	2.47	35	3.36×10^{-3}
12	2.37	36	1.59×10^{-3}
13	2.35	37	4.54×10^{-4}
14	2.23	38	2.14×10^{-4}
15	1.92	39	1.01×10^{-4}
16	1.65	40	3.73×10^{-5}
17	1.35	41	1.07×10^{-5}
18	1.00	42	5.04×10^{-6}
19	0.821	43	1.86×10^{-6}
20	0.743	44	8.76×10^{-7}
21	0.608	45	4.14×10^{-7}
22	0.498	46	1.00×10^{-7}
23	0.369	47	0.00
24	0.298		

[a] Note: The upper energy of Group 1 is 17.33 MeV.

TABLE 6-2
NUCLEAR CONSTANTS FOR NEUTRON FLUX MONITORS CONTAINED IN THE TROJAN SURVEILLANCE CAPSULES

Monitor Material	Reaction of Interest	Target Weight Fraction	Product Half-Life	Fission Yield (%)
Copper	$Cu^{63}(n,\alpha)Co^{60}$	0.6917	5.27 years	
Iron	$Fe^{54}(n,p)Mn^{54}$	0.0585	312 days	
Nickel	$Ni^{58}(n,p)Co^{58}$	0.6777	71.4 days	
Uranium-238[a]	$U^{238}(n,f)Cs^{137}$	1.0	30.2 years	6.0
Neptunium-237[a]	$Np^{237}(n,f)Cs^{137}$	1.0	30.2 years	6.5
Cobalt-Aluminum[a]	$Co^{59}(n,\gamma)Co^{60}$	0.0015	5.27 years	
Cobalt-Aluminum	$Co^{59}(n,\gamma)Co^{60}$	0.0015	5.27 years	

[a] Denotes that monitor is cadmium-shielded.

TABLE 6-3
CALCULATED FAST NEUTRON FLUX (E > 1.0 MeV) AND LEAD FACTOR FOR TROJAN SURVEILLANCE CAPSULES

Capsule	**Azimuthal** Location (deg)	ϕ(E > 1.0 MeV) (n/cm^2-sec)	Lead Factor
U	56°	1.36×10^{11}	4.76
W	124°		
X	236°		
Z	304°		
V	58.5°	1.16×10^{11}	4.06
Y	238.5°		

TABLE 6-4
CALCULATED NEUTRON ENERGY SPECTRA AT THE CENTER OF THE TROJAN SURVEILLANCE CAPSULE X

Group No.	ϕ(n/cm^2-sec)	Group No.	ϕ(n/cm^2-sec)
1	2.23×10^7	25	7.89×10^{10}
2	8.19×10^7	26	8.22×10^{10}
3	2.85×10^8	27	6.61×10^{10}
4	5.22×10^8	28	4.63×10^{10}
5	8.72×10^8	29	1.39×10^{10}
6	1.93×10^9	30	7.47×10^9
7	2.69×10^9	31	2.05×10^{10}
8	5.56×10^9	32	1.32×10^{10}
9	5.18×10^9	33	2.33×10^{10}
10	4.34×10^9	34	3.41×10^{10}
11	5.23×10^9	35	5.79×10^{10}
12	2.62×10^9	36	5.21×10^{10}
13	8.06×10^8	37	7.29×10^{10}
14	4.06×10^9	38	3.96×10^{10}
15	1.09×10^{10}	39	4.40×10^{10}
16	1.49×10^{10}	40	5.95×10^{10}
17	2.33×10^{10}	41	7.03×10^{10}
18	5.28×10^{10}	42	$3,89 \times 10^{10}$
19	4.07×10^{10}	43	4.44×10^{10}
20	1.92×10^{10}	44	2.75×10^{10}
21	7.09×10^{10}	45	2.12×10^{10}
22	5.56×10^{10}	46	2.99×10^{10}
23	6.95×10^{10}	47	3.81×10^{10}
24	6.78×10^{10}		

TABLE 6-5
SPECTRUM AVERAGED REACTION CROSS-SECTIONS AT THE CENTER OF TROJAN SURVEILLANCE CAPSULE X

Reaction	$\bar{\sigma}$ (barns)
$Fe^{54}(n,p)Mn^{54}$	0.0559
$Cu^{63}(n,\alpha)Co^{60}$	0.000479
$Ni^{58}(n,p)Co^{58}$	0.0779
$Np^{237}(n,f)Cs^{137}$	3.338
$U^{238}(n,f)Cs^{137}$	0.313
$Co^{59}(n,\gamma)\ Co^{60}$	24

$$\bar{\sigma} = \frac{\int_0^{\infty} \sigma(E)\ \phi\ (E)dE}{\int_{1.0\ MeV}^{\infty} \phi(E)dE}$$

TABLE 6-6
IRRADIATION HISTORY OF SURVEILLANCE CAPSULES REMOVED FROM THE TROJAN REACTOR

Month	Year	P_{AVG} (MW)	P_{REF} (MW)	P_{AVG}/P_{REF}	Irradiation Time (Days)	Decay[a] Time (Days)	
12	1975	34	3411	0.010	17	3303	
1	1976	205	3411	0.060	31	3272	
2	1976	495	3411	0.145	29	3243	
3	1976	92	3411	0.027	31	3212	
4	1976	819	3411	0.240	30	3182	
5	1976	1283	3411	0.376	31	3151	
6	1976						*THROUGH*
8	1976	0	3411	0.000	92	3059	
9	1976	1504	3411	0.441	30	3029	
10	1976	965	3411	0.283	31	2998	
11	1976	1627	3411	0.477	30	2968	
12	1976	3303	3411	0.969	31	2937	
1	1977	3049	3411	0.894	31	2906	
2	1977	3152	3411	0.924	28	2878	
3	1977						*THROUGH*
6	1977	1422	3411	0.417	122	2756	
7	1977	2855	3411	0.837	31	2725	
8	1977	3087	3411	0.905	31	2694	
9	1977	2333	3411	0.684	30	2664	
10	1977	2957	3411	0.867	31	2633	
11	1977	3281	3411	0.962	30	2603	
12	1977	2875	3411	0.843	31	2572	
1	1978	3319	3411	0.973	31	2541	
2	1978	2869	3411	0.841	28	2513	
3	1978	1460	3411	0.428	31	2482	Capsule U Withdrawn
4	1978						*THROUGH*
12	1978	0	3411	0.000	275	2207	
1	1979	3032	3411	0.889	31	2176	
2	1979	3411	3411	1.00	28	2148	
3	1979	3411	3411	1.00	31	2117	
4	1979	2920	3411	0.856	30	2087	
5	1979						*THROUGH*
6	1979	0	3411	0.000	61	2026	
7	1979	2742	3411	0.804	31	1995	
8	1979	3360	3411	0.985	31	1964	
9	1979	2985	3411	0.875	30	1934	
10	1979	1146	3411	0.336	31	1903	
11	1979	0	3411	0.000	30	1873	
12	1979	7	3411	0.002	31	1842	

TABLE 6-6 (Continued)
IRRADIATION HISTORY OF SURVEILLANCE CAPSULES
REMOVED FROM THE TROJAN REACTOR

Month	Year	P_{AVG} (MW)	P_{REF} (MW)	P_{AVG}/P_{REF}	Irradiation Time (Days)	Decay[a] Time (Days)
1	1980	3186	3411	0.934	31	1811
2	1980	3090	3411	0.906	29	1782
3	1980	2214	3411	0.649	31	1751
4	1980	754	3411	0.221	30	1721
5	1980					THROUGH
6	1980	0	3411	0.000	61	1660
7	1980	938	3411	0.275	31	1629
8	1980	3196	3411	0.937	31	1598
9	1980	3404	3411	0.998	30	1568
10	1980	3363	3411	0.986	31	1537
11	1980	3401	3411	0.997	30	1507
12	1980	3049	3411	0.894	31	1476
1	1981	2974	3411	0.872	31	1445
2	1981	1907	3411	0.559	28	1417
3	1981	3411	3411	1.00	31	1386
4	1981	3220	3411	0.944	30	1356
5	1981	68	3411	0.020	31	1325
6	1981	0	3411	0.000	30	1295
7	1981	1088	3411	0.319	31	1264
8	1981	3169	3411	0.929	31	1233
9	1981	3346	3411	0.981	30	1203
10	1981	2422	3411	0.710	31	1172
11	1981	3350	3411	0.982	30	1142
12	1981	3343	3411	0.980	31	1111
1	1982	2562	3411	0.751	31	1080
2	1982	3186	3411	0.934	28	1052
3	1982	2470	3411	0.724	31	1021
4	1982					THROUGH
7	1982	0	3411	0.000	122	899
8	1982	590	3411	0.173	31	868
9	1982	2923	3411	0.857	30	838
10	1982	3411	3411	1.00	31	807
11	1982	2698	3411	0.791	30	777
12	1982	3411	3411	1.00	31	746
1	1983	2231	3411	0.654	31	715
2	1983					THROUGH
6	1983	0	3411	0.000	150	565
7	1983	467	3411	0.137	31	534
8	1983	1985	3411	0.582	31	503
9	1983	3237	3411	0.949	30	473

TABLE 6-6 (Continued)
IRRADIATION HISTORY OF SURVEILLANCE CAPSULES REMOVED FROM THE TROJAN REACTOR

Month	Year	P_{AVG} (MW)	P_{REF} (MW)	P_{AVG}/P_{REF}	Irradiation Time (Days)	Decay[a] Time (Days)
10	1983	3303	3411	0.970	31	442
11	1983	3411	3411	1.00	30	412
12	1983	3363	3411	0.986	31	381
1	1984	3350	3411	0.982	31	350
2	1984	3114	3411	0.913	29	321
3	1984	3200	3411	0.938	31	290
4	1984	3086	3411	0.905	27	263 Capsule X Withdrawn

Total irradiation time = 1.35×10^{8} EFPS

a) Decay time is referenced to the counting date of the flux monitors (1-15-85).

TABLE 6-7
COMPARISON OF MEASURED AND CALCULATED FAST NEUTRON FLUX MONITOR SATURATED ACTIVITIES FOR CAPSULE X

Reaction and Axial Position	Radial Location (cm)	Saturated Activity (dps/gm)	
		Capsule X	Calculated
$Fe^{54}(n,p)Mn^{54}$			
Top	207.31	4.04×10^6	
Middle	207.31	4.20×10^6	
Bottom	207.31	4.24×10^6	
Average		4.16×10^6	4.97×10^6
$Cu^{63}(n,\alpha)Co^{60}$			
Top	207.31	3.98×10^5	
Middle	207.31	4.15×10^5	
Bottom	207.31	4.15×10^5	
Average		4.09×10^5	4.31×10^5
$Ni^{58}(n,p)Co^{58}$			
Top	207.31	6.07×10^7	
Middle	207.31	6.37×10^7	
Bottom	207.31	6.40×10^7	
Average		6.28×10^7	7.47×10^7
$Np^{237}(n,f)Cs^{137}$			
Middle	207.31	7.30×10^7	7.46×10^7
$U^{238}(n,f)Cs^{137}$			
Middle	207.31	9.03×10^6	6.47×10^6

TABLE 6-8
RESULTS OF FAST NEUTRON DOSIMETRY FOR CAPSULE X

Reaction	Adjusted Saturated Activity (DPS/gm)		Φ (E > 1.0 MeV) (n/cm^2-sec)		$\bar{\Phi}$ (E > 1.0 MeV) (n/cm^2)	
	Measured	Calculated	Measured	Calculated	Measured	Calculated
$Fe^{54}(n,p)Mn^{54}$	4.16×10^6	4.97×10^6	1.15×10^{11}	1.36×10^{11}	1.55×10^{19}	1.84×10^{19}
$Cu^{63}(n,\alpha)Co^{60}$	4.09×10^5	4.31×10^5	1.30×10^{11}	1.36×10^{11}	1.76×10^{19}	1.84×10^{19}
$Ni^{58}(n,p)Co^{58}$	6.28×10^7	7.47×10^7	1.14×10^{11}	1.36×10^{11}	1.54×10^{19}	1.84×10^{19}
$Np^{237}(n,f)Cs^{137}$	7.30×10^7	7.46×10^7	1.33×10^{11}	1.36×10^{11}	1.80×10^{19}	1.84×10^{19}
$U^{238}(n,f)Cs^{137}$	$7.68 \times 10^{6[a]}$	6.47×10^6	$1.61 \times 10^{11[a]}$	1.36×10^{11}	$2.17 \times 10^{19[a]}$	1.84×10^{19}

a. U^{238} adjusted saturated activity has been multiplied by 0.85 to correct for 350 ppm U^{235} impurity.

TABLE 6-9
RESULTS OF THERMAL NEUTRON DOSIMETRY FOR CAPSULE X

Axial Location	Saturated Activity (dps/gm)		
	Bare	Cd-covered	ϕ_{Th} (n/cm^2-sec)
Top	1.26×10^8	6.47×10^7	1.66×10^{11}
Middle	1.14×10^8	6.06×10^7	1.45×10^{11}
Bottom	1.20×10^8	6.31×10^7	1.55×10^{11}
Average	1.20×10^8	6.28×10^7	1.55×10^{11}

TABLE 6-10
SUMMARY OF FAST NEUTRON DOSIMETRY RESULTS FOR CAPSULE X

Basis	Irradiation Time (EFPS)	$\Phi(E > 1.0$ MeV) (n/cm^2-sec)	$\Phi(E > 1.0$ MeV) (n/cm^2)	Lead Factor	Vessel Fluence (n/cm^2)	Calculated Vessel Fluence (n/cm^2)
$Fe^{54}(n,p)Mn^{54}$	1.35×10^8	1.15×10^{11}	1.55×10^{19}	4.76	3.26×10^{18}	3.87×10^{18}
Avg. of all Dosimeters	1.35×10^8	1.31×10^{11}	1.77×10^{19}	4.76	3.72×10^{18}	3.87×10^{18}

TABLE 6-11
CALCULATED CURRENT AND EOL VESSEL EXPOSURE FOR TROJAN

Location	Current Φ (E > 1.0 MeV) (n/cm^2) Calculated	EOL Φ (E > 1.0 MeV) (n/m^2) Calculated
Vessel IR	3.87×10^{18}	2.89×10^{19}
Vessel ¼T	2.22×10^{18}	1.65×10^{19}
Vessel ¾T	4.48×10^{17}	3.35×10^{18}

Note: EOL fluences are based on operation at 3411 MWt for 32 effective full power years.

SECTION 7
SURVEILLANCE CAPSULE REMOVAL SCHEDULE

The following removal schedule is recommended for future capsules to be removed from the Trojan reactor vessel.

Capsule	Lead Factor	Removal Time[a]	Estimated Fluence (10^{19}n/cm^2)
U	4.76	1.23	0.388 (Actual)
X	4.76	4.28	1.77 (Actual)
V	4.06	8	2.93[b]
Y	4.06	15	5.5
W	4.76	Standby	—
Z	4.76	Standby	—

a. EFPY from plant startup

b. Approximate vessel end of life inner wall location fluence

SECTION 8
REFERENCES

1. Davidson, J. A., Phillips, J. H., and Yanichko, S. E., "Portland General Electric Company Trojan Unit 1 Reactor Vessel Radiation Surveillance Program," WCAP-8426, January, 1975.

2. ASTM Standard E185-73, "Recomended Practice for Surveillance Tests for Nuclear Reactor Vessels" in ASTM Standards, Part 10 (1973), American Society for Testing and Materials, Philadelphia, Pa. 1973.

3. Davidson, J. A., Anderson, S. L., and Kaiser, W. T., " Analysis of Capsule U from Portland General Electric Company Trojan Reactor Vessel Radiation Surveillance Program," WCAP-9469, May 1979.

4. Regulatory Guide 1.99, Revision 1, "Effects of Residual Elements on Predicted Radiation Damage to Reactor Vessel Materials," U.S. Nuclear Regulatory Commission, April 1977.

5. Soltesz, R. G., Disney, R. K., Jedruch, J., and Zeigler, S. L., "Nuclear Rocket Shielding Methods, Modification, Updating and Input Data Preparation. Vol. 5 - Two-Dimensional Discrete Ordinates Transport Technique," WANL-PR(LL)034, Vol. 5, August 1970.

6. SAILOR RSIC Data Library Collection "DLC-76, Coupled, Self-shielded, 47 Neutron 20 Gamma-ray, P3, Cross Section Library for Light Water Reactors."

7. Benchmark Testing of Wesinghouse Neutron Transport Analysis Methodology — to be published.

REFERENCES (cont)

8. ASTM Designation E261-77, Standard Method for Determining Neutron Flux, Fluence, and Spectra by Radioactivation Techniques," in ASTM Standards (1983), Section 12, Nuclear Standards, pp. 76-87, American Society for Testing and Materials, Philadelphia, Pa., 1983.

9. ASTM Designation E262-77, Standard Method for Measuring Thermal Neutron Flux by Radioactivation Techniques," in ASTM Standards (1983), Section 12, Nuclear Standards, pp. 88-96, American Society for Testing and Materials, Philadelphia, Pa., 1983.

10. ASTM Designation E263-82, "Standard Method for Determining Fast-Neutron Flux Density by Radioactivation of Iron," in ASTM Standards (1983), Section 12, Nuclear Standards, pp. 97-102, American Society for Testing and Materials, Philadelphia, Pa., 1983.

11. ASTM Designation 481-78, "Standard Method of Measuring Neutron-Flux Density by Radioactivation of Cobalt and Silver," in ASTM Standards (1983), Section 12, Nuclear Standards, pp. 228-235, American Society for Testing and Materials, Philadelphia, Pa., 1983.

12. ASTM Designation E264-82, "Standard Method for Determining Fast-Neutron Flux Density by Radioactivation of Nickel," in ASTM Standards (1983), Section 12, Nuclear Standards, pp. 103-107, American Society for Testing and Materials, Philadelphia, Pa., 1983.